

## Chapter 5

# Oxidation of Proteins by DNA-Mediated Charge Transport

## 5.1 Introduction

### 5.1.1 DNA-mediated CT in a Biological Context

Studies of DNA-mediated Charge Transport (CT) in well-defined molecular assemblies have been enlightening. A large body of work involving metal complex probes bound to short DNA oligomers shapes our current understanding of the factors that affect the efficiency of CT, including the extent of electronic coupling of the probe to the DNA base stack, the thermodynamic driving force for the forward CT reaction to occur, and the probability for the reverse reaction (back electron transport, BET) to take place.<sup>1</sup> These studies have also led to the development of a mechanistic model for CT: injected charge exists within the base stack as a delocalized molecular orbital spanning several neighboring DNA bases, and translocation of the charge through the base stack to low potential redox targets depends on the transient formation of these delocalized domains, defined by conformational fluctuations of the duplex.<sup>1</sup>

Because the motion of charge relies on the stable formation of orbitals spanning several stacked bases, any structural disruption intervening between a charge donor and a charge acceptor decreases the efficiency of DNA-mediated CT. For example, experiments conducted at DNA monolayers on gold surfaces have shown that most base pair mismatches and many naturally occurring base lesions attenuate CT.<sup>2-4</sup> Biochemical and electrochemical experiments have also illustrated the effects that protein binding has on DNA-mediated CT. Proteins that can disrupt the DNA base stack decrease the yield of CT upon binding. Examples include the methyltransferase *M.HhaI*, which flips its target base out of the base stack during methylation, replacing it with glutamine 237, and the restriction endonuclease *R.PvuII*, a TATA binding protein that severely kinks DNA.<sup>5-9</sup> Alternatively, binding of the transcription factor Antennapedia homeodomain protein, which does not distort the base stack upon binding and promotes a slight increase in long-range DNA-mediated CT, most likely due to compaction and rigidification of the bases.<sup>6</sup> Significantly, mutation of glutamine 237 to tryptophan in *M.HhaI* restores long-range CT, proving that protein-induced structural perturbations to the base stack can attenuate DNA-mediated CT.<sup>5,10</sup>

While *in vitro* experiments involving DNA-binding proteins can illustrate the varied

effects of macromolecule binding on DNA-mediated CT, their inclusion does not properly model the plethora of interactions encountered by DNA within the cellular milieu. Several experiments were conducted to study CT in such environments. In particular, a series of experiments were carried out to show that DNA-mediated CT is not inhibited by nucleosome packing and that it can occur over biologically relevant distances. In one such experiment,  $[\text{Rh}(\text{phi})_2(\text{bpy})]^{3+}$  (phi = phenanthrenequinone diimine; bpy = 2,2'-bipyridine) was tethered to the end of a 146 base pair strand of DNA that was wrapped around a histone core. Excitation of the Rh complex resulted in oxidative DNA damage at low potential 5'-GG-3' sites over a distance of 24 base pairs, indicating that nucleosome formation does not inhibit DNA-mediated CT.<sup>11</sup> In another set of experiments, nuclei isolated from HeLa cells were treated with the non-covalent Rh complex and irradiated. In this case, damage was primarily observed at the 5'-G of 5'-GG-3' and 5'-GGG-3' sites, even in protein-bound regions that are not accessible to Rh.<sup>12</sup> In a set of related experiments, oxidative damage in mitochondrial DNA generated by nonspecifically-bound Rh complex was found mainly in conserved sequence block II, a region of the mitochondrial genome responsible for transcriptional regulation.<sup>13-15</sup> Funneling of damage to this particular site is presumed to be evolutionarily advantageous; under conditions of oxidative stress, highly damaged mitochondria cease reproduction. This prevents the propagation of genetic errors, thus maintaining proper metabolic function within the cell. DNA-mediated CT is therefore not only possible within a cell, but it may also be advantageous.

### 5.1.2 Evidence for DNA-Mediated Protein Oxidation

The experiments discussed above show that DNA-mediated CT can occur over long distances and in complex cellular environments. It is therefore not unreasonable that nature could utilize this remarkable phenomenon to perform long-range redox chemistry. Early experiments supporting this proposition involved the use of the flash-quench technique to generate tryptophan cation radicals in DNA-bound tripeptides.<sup>16,17</sup> The flash-quench technique involves the generation of a strong Ru(III) ground state oxidant *in situ* following oxidative quenching of the Ru(II)\* excited state by a diffusible quencher. When this

method is used with  $[\text{Ru}(\text{bpy})_2(\text{dppz})]^{2+}$  or  $[\text{Ru}(\text{phen})_2(\text{dppz})]^{2+}$  (dppz = dipyrido[3,2-*a*:2',3'-*c*]phenazine; phen = 1,10-phenanthroline), the resulting Ru(III) species is strong enough to oxidize guanine or tryptophan. In solutions of Ru(II), quencher, DNA, and the tripeptide Lys-Trp-Lys, photoexcitation of the Ru complex resulted in oxidation of intercalated tryptophan, which was observed by transient absorption (TA) spectroscopy. A similar experiment was carried out with wild-type *M.HhaI* and the Q237W mutant in place of the tripeptide. When the wild-type protein was added to solution, the only transient absorption signal observed belonged to the Ru(III) species. When the mutant was used instead, a transient signal appeared that was assigned to formation of the intercalated tryptophan cation radical.<sup>10</sup> DNA-mediated oxidation of bound proteins is possible even in the absence of an intercalating moiety. In a guanine oxidation assay involving the covalently-bound DNA photooxidant anthraquinone and the DNA-binding cell cycle regulator p53, protein oxidation was attenuated with the introduction of a disruptive base pair mismatch intervening between anthraquinone and p53.<sup>18</sup> In addition, mass spectra of the protein are consistent with the oxidative formation of disulfide bonds generated as a result of DNA-mediated CT. These results show that long-range redox reactions can occur through DNA to form highly reactive amino acid radicals and disulfide bonds within proteins.

Proteins that are known to be redox active can also be oxidized via DNA-mediated CT. In particular, the redox reactivities of the iron-sulfur cluster-containing base excision repair (BER) proteins MutY and endonuclease III (EndoIII) have been studied electrochemically on DNA-modified electrodes. In the absence of DNA, oxidation of the  $[\text{4Fe-4S}]^{2+}$  cluster of EndoIII can be effected by addition of ferricyanide or by application of a +250 mV electrochemical potential. Under these conditions, oxidation of the cluster is irreversible and degradative, resulting in formation of the  $[\text{3Fe-4S}]^+$  product.<sup>19,20</sup> In the presence of DNA, reversible oxidation occurs at a potential of  $\sim 50$  mV vs. NHE, forming the  $[\text{4Fe-4S}]^{3+}$  cluster.<sup>20,21</sup> DNA binding, therefore, stabilizes the 3+ form of the cluster. The behavior of MutY, which is highly homologous to EndoIII and also contains a  $[\text{4Fe-4S}]^{2+}$  cluster, is similar. Oxidation of this protein on a DNA-modified gold electrode gives a redox potential of 90 mV vs. NHE.<sup>21,22</sup> DNA binding was also observed to dramatically shift the

redox potential of the transcription factor SoxR.<sup>23</sup> In the absence of DNA, the oxidation potential of the protein is  $-290$  mV vs. NHE. In the presence of DNA, this potential shifts by over  $+450$  mV to  $+200$  mV vs. NHE. These results indicate that DNA binding greatly influences the reactivity of these redox-active enzymes. For the BER proteins, the DNA binding affinity is expected to increase by several orders of magnitude upon oxidation of the [4Fe-4S] cluster from the  $2+$  to the  $3+$  state.<sup>20</sup> These proteins therefore bind more tightly to DNA in an oxidizing environment, where oxidative base lesions are more likely to form. In the case of SoxR, the shift in potential may instead provide the energy to bend DNA. Such a conformational change induced by SoxR binding has been observed in copper phenanthroline footprinting experiments.<sup>23</sup> In photooxidation experiments involving SoxR and  $[\text{Rh}(\text{phi})_2(\text{bpy})]^{3+}$  tethered to DNA, activation of transcription could be accomplished *in vitro* by long-range DNA-mediated CT over a distance of 80 base pairs ( $270$  Å).<sup>24</sup> The results of these experiments indicate that oxidation of redox-active enzymes may serve to direct the biological functions of BER protein activation and transcriptional activation.

### 5.1.3 Evidence Supporting Redox Signaling by DNA-mediated CT

Mounting experimental evidence suggests that DNA-mediated CT may play another role in the mechanism of action of BER enzymes, namely, as the method by which these enzymes detect genetic damage. The observation of long-range CT in guanine oxidation experiments<sup>25</sup>, the physiologically relevant redox potentials of DNA-bound BER proteins, the elimination of DNA-mediated CT in strands containing base mismatches or lesions, and the ability of these iron-sulfur proteins to participate in DNA-mediated CT systems as oxidative traps suggest that these proteins could scan large stretches of the genome for damage simply and efficiently by passing a charge through it.

A model has been proposed to illustrate the mechanism of lesion detection by BER enzymes (Figure 5.1).<sup>22</sup> First, one protein with a  $[\text{4Fe-4S}]^{2+}$  cluster binds to DNA and becomes oxidized, perhaps via hole transfer from a nearby guanine radical generated by ROS. The protein, now with an oxidized  $[\text{4Fe-4S}]^{3+}$  cluster, remains tightly bound to the duplex. If a second protein with a  $[\text{4Fe-4S}]^{2+}$  cluster binds nearby, CT can occur through

the base stack between the two bound proteins. This CT event comprises a scan of the genomic region for base lesions. Following CT, the first protein, now bearing a 2+ cluster, can dissociate, and the process repeats. In the event that a mismatch or lesion intervenes between two bound proteins, CT cannot occur. In this case, both proteins will remain bound, precessing more slowly to the damage site.

Importantly, this DNA-mediated search for damage can be performed cooperatively between any two proteins with redox potentials of approximately 100 mV. Support for cooperative searching has been established using a number of different approaches.<sup>26</sup> First, computational models show that if 20% of BER enzymes are oxidized and CT is allowed over distances of 200 base pairs, a search of the full *E. coli* genome would take only 8 minutes. As a comparison, a simpler model involving only facilitated diffusion requires 46 minutes. Considering that the doubling time of *E. coli* is only 20 minutes, it is clear that facilitated diffusion is inadequate; many lesions would be left unrepaired. Second, atomic force microscopy experiments show that proteins are bound more often to DNA strands containing a mismatch than to well-matched strands. Remarkably, this effect is statistically significant even when mismatch strands are used that contain only one mismatched base pair out of 3,800. Third, a transversion assay was used to test the ability of different BER enzymes to help one another search for lesions. In *E. coli* EndoIII knockouts, repair of the target lesion of MutY was only 50% as efficient as in the fully functional reporter strain. These results collectively strengthen the argument for a cooperative DNA-mediated search mechanism involving redox active proteins.

#### **5.1.4 Time-Resolved Spectroscopy with Redox-Active Proteins**

While biochemical and electrochemical experiments have been useful in elucidating the role that DNA-mediated CT may play in biological processes, these methods cannot be used to characterize the rates or absolute efficiencies of such processes. Spectroscopic methods, however, can be used to observe specific products as they form. By monitoring the emission or absorption of a sample over time, it is often possible to observe short-lived reactive or unstable chemical species. Such techniques have already been used to observe the guanine

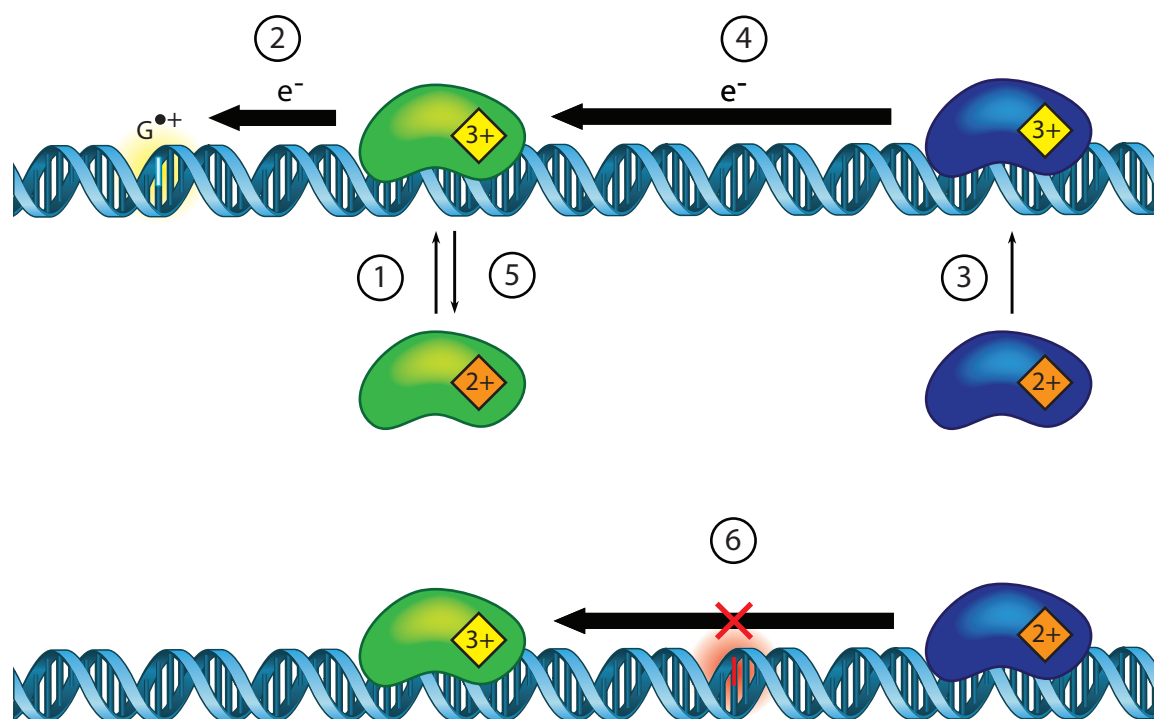


**Figure 5.1:** A model for the DNA-mediated detection of lesions. 1) A protein containing a  $[4\text{Fe-4S}]^{2+}$  cluster binds to DNA. 2) Electron transfer to a nearby guanine cation radical results in formation of the  $[4\text{Fe-4S}]^{3+}$  cluster. The protein is now strongly bound to the DNA strand. 3) A second protein, which contains a  $[4\text{Fe-4S}]^{2+}$  cluster, binds nearby. 4) CT between the two proteins comprises a scan of the region for DNA damage. 5) The protein now bearing the 2+ cluster dissociates and the process repeats. 6) If a lesion intervenes between the proteins, CT cannot occur, and the proteins proceed to the location of the damage.

cation radical, formed in poly(dG-dC) using the flash-quench technique.<sup>27</sup> In this experiment, the guanine radical persisted for milliseconds, depending on the quencher employed. The DNA-mediated oxidation of metalloproteins has also been observed spectroscopically. In the presence of DNA and ferricytochrome *c*, excitation of  $[\text{Ru}(\text{phen})_2(\text{dppz})]^{2+}$  results in the formation of the reduced protein.<sup>28</sup> Similarly, the flash-quench technique can be used to oxidize MutY. In this experiment, the formation of a long-lived, positive transient absorption band near 410 nm was assigned to the oxidized  $[\text{4Fe-4S}]^{3+}$  cluster of the protein.<sup>29</sup> Importantly, the guanine cation radical was an intermediate in the protein oxidation reaction in both cases. This similarity suggests that the guanine radical may play a general role as a redox intermediate in biochemical pathways involving DNA-mediated oxidation. In addition, it should be stressed that formation of the oxidized proteins in both experiments was observed directly as the reaction was occurring. The ability to directly observe these transient species makes time-resolved spectroscopy the best tool to characterize the DNA-mediated oxidation of redox-active proteins.

Here, we describe several lines of work that share a common goal: to observe the DNA-mediated oxidation of redox-active proteins spectroscopically. Various experimental strategies, detailed below, were employed to this end. Observations in p53 systems are very promising. Although spectra obtained under conditions designed for p53 oxidation are of low intensity and were difficult to reproduce, they compare favorably to transient spectra obtained upon oxidation of tyrosine in Lys-Tyr-Lys tripeptides. Measurements in SoxR systems were hindered by the presence of dithionite. This reducing agent, included to keep the protein in the reduced form, greatly complicated the kinetics of the system. Some evidence suggests that dithionite can serve as a reductive quencher of Ru(II)\* luminescence. The third protein studied is EndoIII. Although no direct evidence for its oxidation was obtained, experiments involving metal complex photooxidants suggest that the addition of EndoIII does introduce an additional sink for oxidative DNA-mediated CT. These results together highlight experimental challenges faced in bioinorganic spectroscopy and provide a foundation on which to base further experiments.

## 5.2 Experimental Section

### 5.2.1 Materials

All materials were purchased from commercial sources and used as received unless otherwise indicated. DNA synthesis reagents were purchased from Glen Research (Sterling, VA). The synthesis of  $[\text{Re}(\text{CO})_3(\text{dppz})(\text{py}')]\text{Cl}$  is described completely in Section 2.2.2 on Page 59. The complexes  $[\text{Ir}(\text{ppy})_2(\text{dppz}')]\text{Cl}$  and  $[\text{Rh}(\text{phi})_2(\text{bpy}')]\text{Cl}_3$  were gifts from coworkers or were prepared using established protocols.<sup>30,31</sup>

### 5.2.2 Synthesis of DNA and Tethered Conjugates

Oligonucleotides were prepared using standard solid-phase phosphoramidite chemistry on an Applied Biosystems 3400 DNA synthesizer. Covalent tethers were appended to the 5'-ends of resin-bound oligonucleotides as described in Section 4.2.3 on page 128. Annealing was accomplished by incubating solutions containing equimolar amounts of complementary strands in buffer (10 mM  $\text{NaP}_i$ , 50 mM NaCl buffer; pH 7.5) at 90 °C for 5 min followed by slow cooling over 90 min to ambient temperature. The melting temperature ( $T_m$ ) of each duplex was determined by monitoring the 260 nm absorbance of a dilute sample while heating slowly (1 °C  $\text{min}^{-1}$ ) from ambient temperature to 100 °C; the  $T_m$  is taken as the inflection point of the melting curve.

### 5.2.3 Protein Expression and Purification

The proteins p53 and SoxR were expressed, purified, and kindly supplied by Wendy Mercer and Paul Lee, respectively. EndoIII was expressed from the pNTH10 expression vector and purified as described.<sup>32</sup> Briefly, pNTH10 was transformed into JM101 cells by electroporation at 1.7 kV. Following selection on LB+ampicillin plates, a large-scale culture was grown to  $\text{OD}_{600} = 0.6\text{--}0.8$ . EndoIII expression was induced by the addition of 0.5 mL 1 M isopropyl- $\beta$ -D-thiogalactopyranoside and incubated at 37 °C for 4 hours. Cells were pelleted, washed, and lysed with lysozyme in the presence of phenylmethylsulfonyl fluoride. Nucleic acids were degraded with DNaseI and RNaseA. Anion exchange on quaternary methylammonium resin (Sigma) and cation exchange on sulfopropyl sepharose resin (Sigma) were

performed at 4 °C to remove nucleic acids and other impurities. The protein was precipitated with ammonium sulfate, resuspended, and purified by size exclusion chromatography (AcA54 resin, Sigma). Purity was determined by SDS-PAGE. Protein solutions were concentrated by reverse dialysis with polyethylene glycol in buffer. Concentrated solutions were dialyzed into storage buffer (20 mM NaP<sub>i</sub>, 100 mM NaCl, 1 mM EDTA, 20% glycerol; pH 7.5) and stored in working aliquots at -80 °C. Protein activity was verified with a glycosylase assay.

### 5.2.4 Time-Resolved Spectroscopy

Time-resolved spectroscopic experiments were performed at the Beckman Institute Laser Resource Center. Time-resolved emission and TA measurements were conducted using instrumentation that has been described.<sup>33</sup> Briefly, the third harmonic (355 nm) of a 10 Hz, Q-switched Nd:YAG laser (Spectra-Physics Quanta-Ray PRO-Series) was used as an excitation source (pump pulse duration  $\approx$ 8 ns). For the measurement of transient absorbance spectra, a white light flashlamp of  $\sim$ 15 ns duration was employed as the probe lamp, and two photodiode arrays (Ocean Optics S1024DW Deep Well Spectrometer) detected the measurement and reference beams. For the measurement of transient kinetics, the probe light was provided by a pulsed 75 W arc lamp (PTI model A 1010) and detected with a photomultiplier tube (Hamamatsu R928) following wavelength selection by a double monochromator (Instruments SA DH-10). For both spectral and kinetic measurements, the pump and probe beams were collinear, and scattered laser light was rejected from the detectors using suitable filters. The samples were held in 1-cm-path-length quartz cuvettes (Starna) equipped with stir bars and irradiated at 355 nm with 500–1000 laser pulses at 5 mJ pulse<sup>-1</sup>. Samples were monitored for degradation by UV/visible absorbance and exchanged for fresh sample when necessary. Samples were prepared with a maximum absorbance of 0.8 in order to achieve high signal-to-noise ratios in TA experiments. TA measurements were made with and without excitation, and were corrected for background light, scattering, and fluorescence. Transient spectra were smoothed using a boxcar algorithm to reduce the effect of instrumental noise. In some cases, additional correction was needed in the form of scaled

blank subtraction.

Kinetic traces were fit to exponential equations of the form

$$I(t) = a_0 + \sum_n a_n \exp(-t/\tau_n),$$

where  $I(t)$  is the signal intensity as a function of time,  $a_0$  is the intensity at long time,  $a_n$  is a pre-exponential factor that represents the relative contribution from the  $n$ th component to the trace, and  $\tau_n$  is the lifetime of the  $n$ th component. Up to two exponential terms were used in the model function to obtain acceptable fits. Kinetic traces were smoothed logarithmically prior to fitting in order to decrease the weight of long time data on the fit.

## 5.3 Results & Discussion

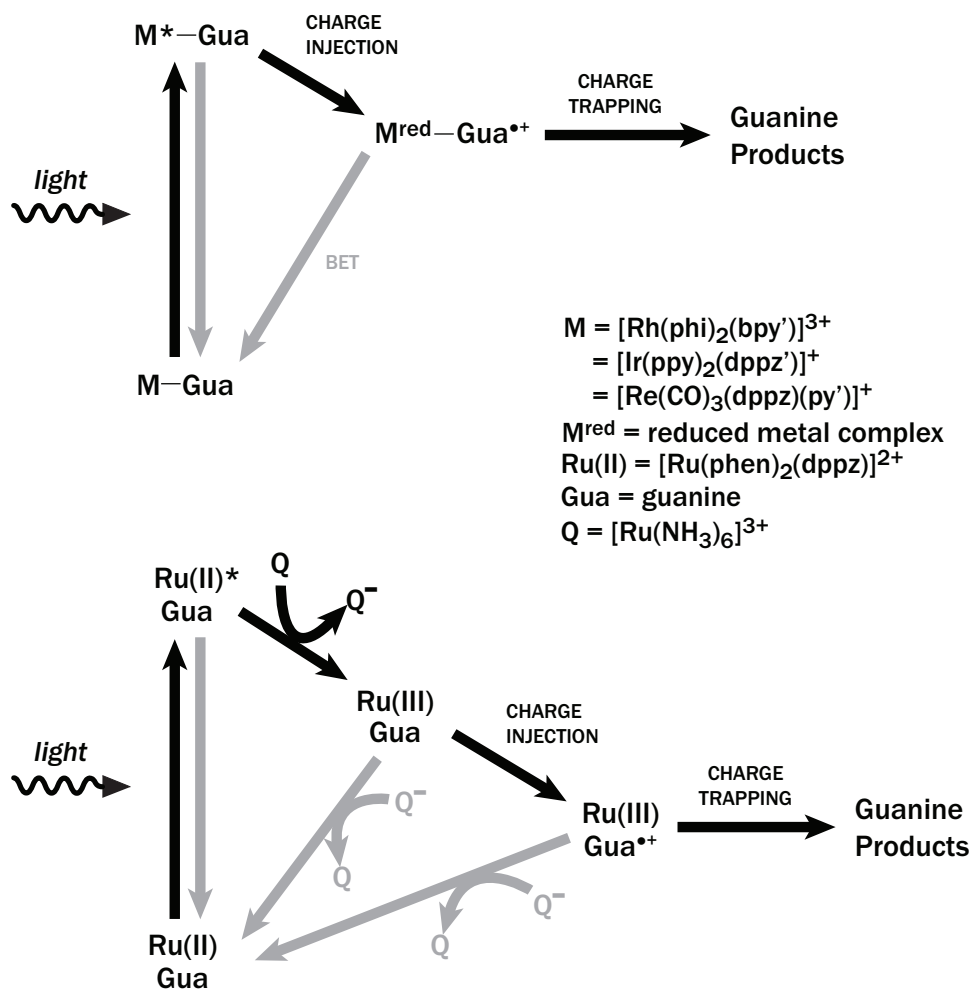
### 5.3.1 Oxidation Strategies

Two strategies for the formation of oxidative damage are shown in Scheme 5.1. Direct photooxidation is the most straightforward way to inject charge into DNA. Generally, photoexcitation of an intercalated metal complex results in the formation of a strong excited state oxidant. Strong electronic coupling between the intercalating ligand and the base stack facilitate efficient charge injection, generating the reduced metal complex and a cation radical within the base stack. DNA-mediated CT to a low potential site such as guanine results in charge localization at the site. Subsequent reaction with water or dioxygen traps the radical, forming a permanent product. The yield of the charge trapped product can be decreased if BET from the target cation to the reduced metal complex is competitive with trapping. This oxidation strategy has been used in numerous experiments to explore the factors affecting the yield of DNA-mediated oxidation. Such factors include distance,<sup>25</sup> oxidation target,<sup>34</sup> DNA structure,<sup>35-38</sup> DNA sequence,<sup>39</sup> and protein binding.<sup>5,6,11,40</sup> This method has also been used to study the repair of thymine dimers,<sup>41,42</sup> to oxidize DNA *in vivo*,<sup>12-15</sup> to oxidize DNA-bound proteins *in vitro*,<sup>18,24</sup> and to compare hole transfer with electron transfer (ET).<sup>43-45</sup>

The flash-quench technique was originally established for the study of intramolecular

ET through proteins. Although mechanistically more complex than direct photooxidation, this method allows for observation of CT rates over an extremely wide range. The mechanism of the oxidative flash-quench method is as follows. Excitation of an intercalated metal complex oxidant is followed by excited state quenching, usually through bimolecular ET with a diffusing quencher such as  $[\text{Ru}(\text{NH}_3)_6]^{3+}$ , methylviologen, or  $[\text{Co}(\text{NH}_3)_5\text{Cl}]^{2+}$ . The resulting ground state species is a strong, long-lived oxidant that can proceed to oxidize the redox target. Again, formation of the target radical is followed by trapping to form a permanent product. The flash-quench method is not limited to oxidative systems; a long-lived Ir ground state reductant has also been prepared using 5-bromouridine as the quencher.<sup>44,45</sup> Like direct photooxidation, the flash-quench technique has been used in a number of experimental systems for guanine oxidation,<sup>25,27,34,46–48</sup> methylindole oxidation,<sup>49–51</sup> peptide and protein oxidation,<sup>10,16,17,24,28,29</sup> and DNA-peptide crosslinking.<sup>52</sup>

These two methods of oxidation appear quite similar. They both involve photoexcitation of the charge donor, and they both result in the formation of permanent oxidative damage at low potential charge acceptors. However, differences in these two mechanisms may make one method more suitable than the other for a particular experiment. For example, charge injection in direct photooxidation occurs rapidly, allowing for the observation of very fast processes. On the other hand, since CT must occur within the lifetime of the excited state, processes with very slow rates, such as tunneling through high potential media or CT over long distances, cannot be observed. Additionally, BET in these systems may be quite facile since the conditions that are conducive to efficient forward CT, such as strong electronic coupling between the donor/acceptor pair and the bridge, also permit efficient BET. In the flash-quench reaction, CT processes with very slow rates can be observed, but diffusion of the quencher limits the study of fast processes. BET in flash-quench systems also behaves differently. Since the donor returns to its initial oxidation state upon charge injection, direct charge recombination is unlikely. The product yield may still be diminished, however, through ET from the reduced quencher. By using a sacrificial quencher such as  $[\text{Co}(\text{NH}_3)_5\text{Cl}]^{2+}$ , even these recombination pathways can be abolished, although additional challenges may be introduced. Therefore, for systems in which very fast processes must be



**Scheme 5.1:** Comparing direct photooxidation and the flash-quench technique. Top, direct photooxidation: excitation of an intercalated metal complex ( $M$ ) results in formation of the metal complex excited state ( $M^*$ ). CT through the DNA base stack causes oxidation of guanine, forming the guanine cation radical ( $G^{\bullet+}$ ). A bound protein can be oxidized by the relatively long-lived guanine radical. BET may occur to neutralize the radical, or reaction with water or oxygen can form permanent oxidized guanine products. Bottom, the flash-quench technique: the excitation of  $[\text{Ru}(\text{phen})_2(\text{dppz})]^{2+}$ ,  $\text{Ru(II)}$ , results in the formation of the excited species  $\text{Ru(II)}^*$ . Oxidative quenching by a diffusing quencher,  $Q$ , forms the ground state oxidation  $\text{Ru(III)}$ .  $\text{Ru(III)}$  proceeds to oxidize guanine. Protein oxidation may result. Here, BET involves reduction by the reduced quencher.

observed, direct photooxidation should be used, but when high product yields are desired, the flash-quench technique is the better option.

### 5.3.2 p53

The protein p53 is a transcriptional regulator that mediates the cellular response to a number of stress signals, including DNA damage, hypoxia, and ribonucleotide depletion.<sup>53,54</sup> Depending on the type and severity of stress, the p53 response may induce apoptosis, senescence, cell cycle arrest, DNA repair, or differentiation. Because of the central role that p53 plays in many cellular pathways, its stability is necessary for cell survival. Single point mutations in the DNA binding core domain are extremely disruptive to protein function. Such mutations are found in over 50% of human cancers. For this reason, a full understanding of the biochemical reactivity of p53 is imperative. Experimental evidence has already shown that p53 can be oxidized via DNA-mediated CT.<sup>18</sup> Knowledge of the specific pathway by which this reaction occurs may help us understand how oxidative stress affects the function of p53.

#### Experimental Details

The 393-amino acid p53 is made up of several domains, including some regions that are natively unfolded.<sup>55</sup> For example, the transactivation domain in the N-terminal region interacts with a number of regulatory proteins. The DNA-binding core domain (residues 94–292) binds specifically as a homotetrameric complex to double-stranded DNA at two “half-site” motifs, each with the sequence 5′-Pu-Pu-Pu-C-(A,T)-(T,A)-G-Py-Py-Py-3′ (Pu = A, G; Py = C, T) separated by up to 13 base pairs.<sup>56</sup> The binding affinity of the p53 complex depends on the DNA sequence. The tetramerization domain is found in the C-terminal region (residues 325–356). Both the N-terminus and C-terminus domains are largely unfolded except in the presence of certain regulatory proteins. The DNA binding domain and the tetrameric domain, on the other hand, have well defined conformations. While the whole protein has defied crystallization, crystal structures of the DNA binding domain and the tetrameric domain have been solved. Even these domains are relatively unstable, with

melting temperatures only slightly above 37 °C.

Because of the low melting temperature and the high degree of disorder in the p53 termini, the expression and study of p53 and destabilizing mutants can be extremely challenging. For this reason, it is often necessary to use mutationally stabilized or truncated versions of the protein in biophysical experiments. In most of the experiments described below, a superstable quadruple mutant, *T*-p53C (4×), was used.<sup>57</sup> This version of p53 contains the mutations M133L, V203A, N239Y, and N268D, and is stabilized versus the wild-type protein by 2.6 kcal mol<sup>-1</sup>. Since the design of this mutant was based on natural variations of p53 in many different species, protein function has been retained. Intriguingly, asparagine 239 in the wild-type protein is in contact with the DNA backbone. It is possible that substitution of this residue for tyrosine in the 4× mutant establishes a CT path into the core of the protein, as was observed for *Pseudomonas aeruginosa* azurin.<sup>58</sup> For this reason, the 3× mutant lacking this mutation was also studied.

Time-resolved spectroscopic experiments were conducted to observe the oxidation of DNA-bound p53 by DNA-mediated CT. The experimental design is shown in Figure 5.2. These studies were based on the experiments of Wagenknecht et al., in which the flash-quench technique was used to generate the tyrosine radical in the DNA-bound Lys-Tyr-Lys tripeptide.<sup>16</sup> In those experiments, the photoexcitation of covalently tethered [Ru(phen)(bpy')(dppz)]<sup>3+</sup> (bpy' = 4-methyl-4'-(butyric acid)-2,2'-bipyridine) resulted in the formation of a strong transient absorbance signal at 405 nm. The growth rate of this signal, ~30 μs, matched the decay rate of guanine cation radical (G<sup>•+</sup>), observed at 510 nm, indicating an intermediating role for the latter species. The decay rate of the tyrosine radical was ~100 μs. Both the rate of formation and the rate of decay of the tyrosine radical were observed to depend on the DNA sequence. Here, formation of the tyrosine radical is also expected upon Ru excitation due to the close proximity of tyrosine 239 to DNA in the 4× mutant. In addition, the DNA sequence included the consensus sequence 5'-AAATCAGCACTACAACATGTTGGGACATGTTC-3' as a putative p53 binding site (promotor region underlined). The oxidation targets in these experiments are adjacent cysteine pairs within the DNA binding domain of p53: cysteines 275 and 277, and cys-

teines 135 and 141.<sup>18</sup> Upon oxidation, these cysteine pairs may form disulfite bonds. The oxidation potential of cysteine is  $\sim 0.42$  V vs. NHE<sup>59</sup>, so it should be easily oxidized using the flash-quench method ( $E^\circ[\text{Ru}^{3+}/\text{Ru}^{2+}] = 1.6$  V vs. NHE;  $E^\circ[\text{G}^{\bullet+}/\text{G}] = 1.29$  V vs. NHE).<sup>60,61</sup>

### Oxidation of Lys-Tyr-Lys

Before examining the DNA-mediated oxidation of p53, it was prudent to repeat the experiments of Wagenknecht et al.<sup>16</sup> regarding the oxidation of the tripeptide Lys-Tyr-Lys. In this way, we could ensure that the current instrumentation would be sufficiently sensitive for experiments involving the protein. Samples were prepared with 750  $\mu\text{M}$  (base pairs) herring testes DNA (42% GC content), 40  $\mu\text{M}$   $[\text{Ru}(\text{phen})_2(\text{dppz})]^{2+}$ , 600  $\mu\text{M}$   $[\text{Ru}(\text{NH}_3)_6]^{3+}$  quencher, and 0 or 600  $\mu\text{M}$  Lys-Tyr-Lys in phosphate buffer (10 mM  $\text{NaP}_i$ , 50 mM NaCl; pH 7.5).

The transient spectrum measured 50  $\mu\text{s}$  after 480 nm excitation is shown in Figure 5.3. In the absence of tripeptide, the transient signal of  $[\text{Ru}(\text{phen})_2(\text{dppz})]^{3+}$  is observed. The bleach centered at 440 nm is due to depletion of the Ru(II) ground state; the transient band that appears at higher wavelengths is typical of the 3+ species. In the presence of tripeptide, the spectrum changes dramatically. An intense positive band appears at 405 nm accompanied by a minor band near 460 nm. No evidence remains for the Ru(II/III) bleach, and the intensity of the low energy transient is very low, suggesting that at these high concentrations, oxidation of the tripeptide is nearly quantitative. This spectrum is almost identical to the one measured by Wagenknecht et al., so it is assigned to the tyrosine cation radical.

While the tyrosine cation radical spectrum can be consistently produced at high intensity using the experimental conditions listed above, it was also necessary to measure this control at the same concentrations and in the same buffer as the p53 experiment. This was a challenging task. In order to maintain stability, the protein must be dissolved in a complex buffer containing many components. In particular, the higher ionic strength and viscosity are expected to diminish the efficiency of charge injection, since a higher ion

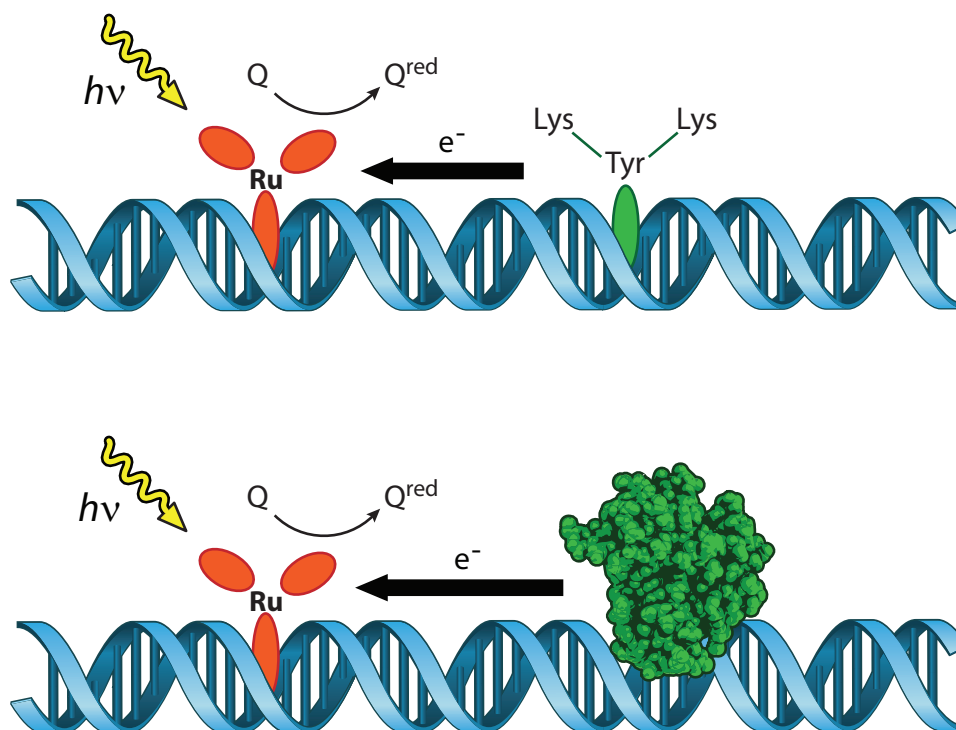


**Figure 5.2:** The p53 transient absorption experiment. Excitation of  $[\text{Ru}(\text{phen})_2(\text{dppz})]^{2+}$  at 470 nm and quenching by  $[\text{Ru}(\text{NH}_3)_6]^{3+}$  (Q) results in formation of  $[\text{Ru}(\text{phen})_2(\text{dppz})]^{3+}$ . This species can oxidize guanine to form the guanine cation radical,  $\text{G}^{\bullet+}$ . Top: hole transfer from  $\text{G}^{\bullet+}$  to Lys-Tyr-Lys results in the formation of the tyrosine cation radical. Bottom: hole transfer from  $\text{G}^{\bullet+}$  to p53 results in the formation of a disulfide bond in the protein.

content will decrease the electrostatic attraction between the Ru(II) oxidant and DNA, and higher viscosity will retard quencher diffusion. Additionally, since p53 solutions are not stable at concentrations higher than approximately 50  $\mu\text{M}$ , low concentrations of tripeptide must be used.

For these reasons, transient absorption spectra were also measured for solutions containing 20  $\mu\text{M}$  consensus sequence DNA (32-mer), 20  $\mu\text{M}$   $[\text{Ru}(\text{phen})_2(\text{dppz})]^{2+}$ , 600  $\mu\text{M}$   $[\text{Ru}(\text{NH}_3)_6]^{3+}$  quencher, and 0 or 50  $\mu\text{M}$  Lys-Tyr-Lys in p53 buffer (20 mM Tris, 100 mM NaCl, 0.2 mM EDTA, 0.1% bovine serum albumin, 0.1% MP-40 detergent, 10% glycerol; pH 8.0). These measurements are shown in Figure 5.4(left). In the absence of tripeptide, the Ru(III) bleach is clearly observed, even at times as long as 75  $\mu\text{s}$  after excitation. With the addition of tripeptide, the change in the spectral profile is modest. At 30 and 50  $\mu\text{s}$ , the bleach and transient due to Ru(III) formation are clearly visible, indicating that much of the oxidant remains unreacted. The main difference is the appearance of a narrow transient band near 405 nm. Despite the noise, this band is observed at all three time points. Based on the transient spectrum observed at a lower salt concentration and a higher tripeptide concentration, this narrow band can be assigned to the tyrosine cation radical as well.

### **Oxidation of p53**

The flash-quench experiment was also conducted with p53. Transient spectra are shown in Figure 5.4 (right) for samples including 20  $\mu\text{M}$   $[\text{Ru}(\text{phen})_2(\text{dppz})]^{2+}$ , 20  $\mu\text{M}$  consensus sequence DNA, 600  $\mu\text{M}$   $[\text{Ru}(\text{NH}_3)_6]^{3+}$  quencher, and 0 or 50  $\mu\text{M}$  p53 in protein buffer following 470 nm excitation. At each time point, the addition of protein results in a decrease in the intensity of the Ru(III) bleach, suggesting that p53 acts as an additional hole sink. In addition, a low intensity transient band appears near 410 nm, which is especially apparent at short times. The position and breadth of this band suggest that it is due to the same process as the positive band in the Lys-Tyr-Lys controls, namely, absorption of the tyrosine cation radical. Its disappearance at long times may indicate further reaction, as is expected for an aromatic residue that lies along the CT pathway to an even stronger low potential trap<sup>58,62</sup>.

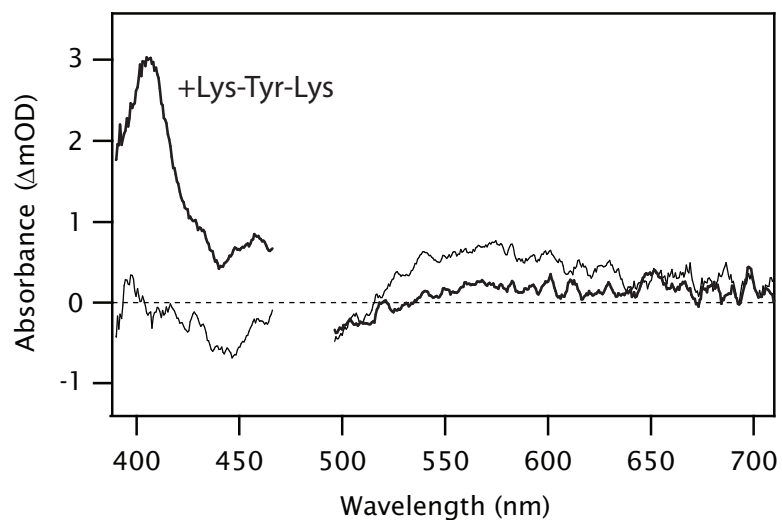


**Figure 5.3:** Transient absorption spectra without (thin) and with (thick) Lys-Tyr-Lys, as done by Wagenknecht, et al.<sup>16</sup> Samples contained 750  $\mu\text{M}$  (base pairs) herring testes DNA (42% GC content), 40  $\mu\text{M}$   $[\text{Ru}(\text{phen})_2(\text{dppz})]^{2+}$ , 600  $\mu\text{M}$   $[\text{Ru}(\text{NH}_3)_6]^{3+}$  quencher, and 0 or 600  $\mu\text{M}$  Lys-Tyr-Lys in phosphate buffer (10 mM  $\text{NaP}_i$ , 50 mM  $\text{NaCl}$ ; pH 7.5). Spectra were measured 50  $\mu\text{s}$  after 480 nm laser excitation. Data between 470 nm and 490 nm were removed due to scatter from the excitation beam.

The spectra shown in Figure 5.4 were the best obtained for this system. Although the experiment was attempted several times and under different sets of conditions, it was not possible to improve the signal. Experiments involving the 3× mutant, which were conducted to determine whether the tyrosine radical observed corresponds to the residue introduced by mutagenesis, were inconsistent. As indicated above, the sample conditions that are necessary to maintain protein stability are not conducive to spectroscopy. While the influences of additional sample components such as EDTA and detergents on interactions between macromolecules and metal complexes are unknown, the effects of unstable proteins are usually worse; precipitated protein scatters pump and probe light, decreasing the signal-to-noise ratio of transient absorption data dramatically. Another challenge is proving that oxidation occurs by DNA-mediated CT. Stability of p53 also requires the presence of DNA, so it is impossible to perform a control experiment in which DNA is absent. Despite these challenges, the results presented above are promising. Based on these data, it appears that the oxidation of p53 can be observed by transient absorption spectroscopy.

### 5.3.3 SoxR

SoxR is a bacterial redox-active transcriptional regulator that contains a [2Fe-2S] cluster.<sup>63</sup> Oxidation of the cluster activates the protein, but it does not affect protein folding, DNA binding, or promoter affinity.<sup>23,64</sup> Following oxidation, the DNA-bound protein is thought to undergo a conformational change, unwinding the promoter for SoxS, a transcription factor that controls the cellular response to oxidative stress. Experiments on DNA-modified gold electrodes have shown that the redox potential of DNA-bound SoxR is 400 mV higher than that of SoxR in solution.<sup>23</sup> In addition, SoxR can be activated by DNA-mediated oxidation *in vitro* and *in vivo* using either a direct photooxidant or the flash-quench technique. In these experiments, indirect evidence for SoxR activation by DNA-mediated oxidation entailed a diminution in guanine oxidation or increased levels of *soxS* transcript upon addition of protein. Observation of oxidized SoxR by time-resolved spectroscopy would provide complementary direct evidence for this process.

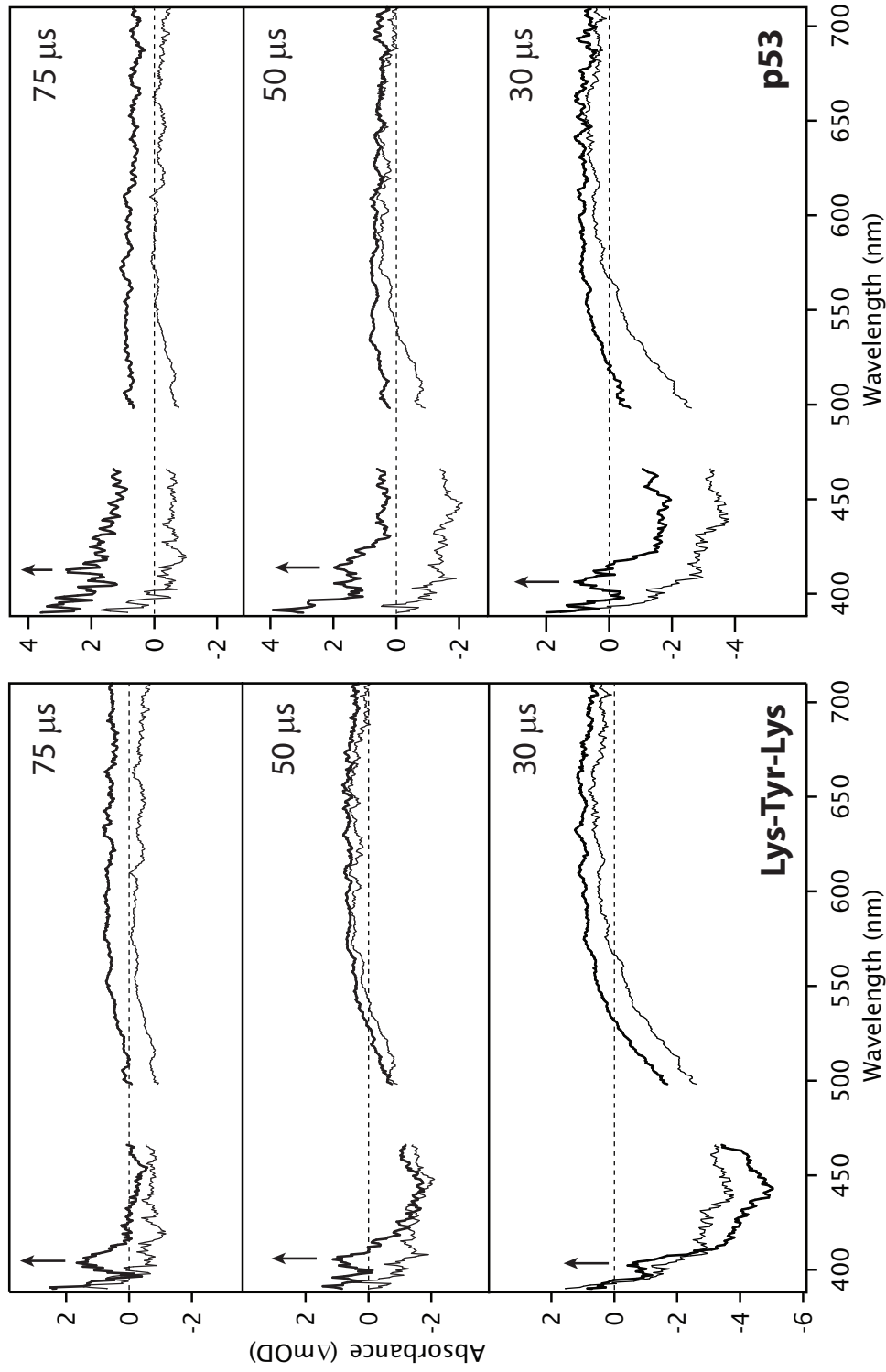


**Figure 5.4:** Transient absorption spectra in the absence (thin) and presence (thick) of Lys-Tyr-Lys (left) or p53 (right). Samples contained 20  $\mu\text{M}$  consensus sequence DNA (32-mer), 20  $\mu\text{M}$   $[\text{Ru}(\text{phen})_2(\text{dppz})]^{2+}$ , 600  $\mu\text{M}$   $[\text{Ru}(\text{NH}_3)_6]^{3+}$  quencher, and 0 or 50  $\mu\text{M}$  Lys-Tyr-Lys or p53 in protein buffer (20 mM Tris, 100 mM NaCl, 0.2 mM EDTA, 0.1% bovine serum albumin, 0.1% MP-40 detergent, 10% glycerol; pH 8.0). Spectra were measured 30, 50, or 75  $\mu\text{s}$  after 470 nm laser excitation, as indicated. Arrows show the direction of change with the addition of protein.

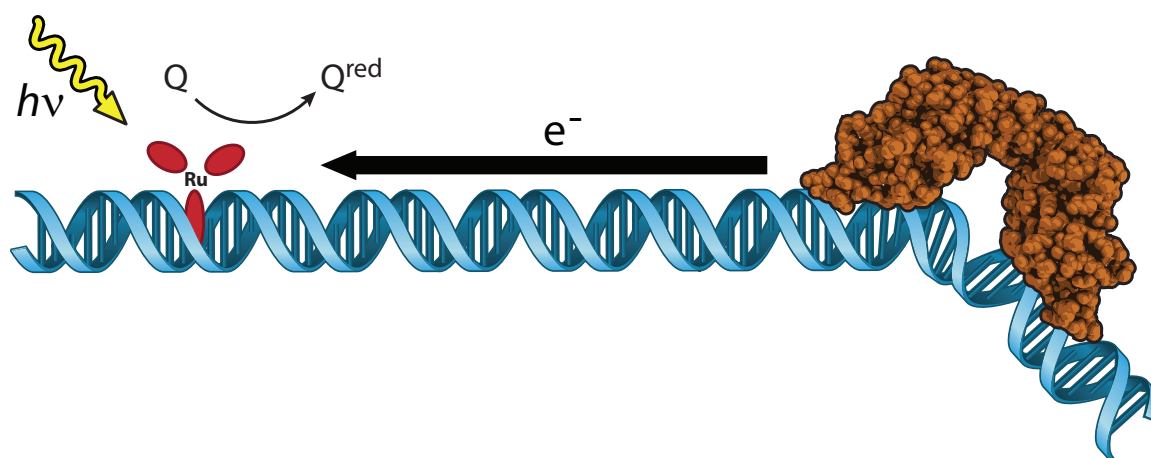
## Experimental Details

The flash-quench method was used in SoxR oxidation experiments. This method has been used previously to show that the addition of SoxR to samples including  $[\text{Ru}(\text{phen})_2(\text{dppz})]^{2+}$ , the sacrificial quencher  $[\text{Co}(\text{NH}_3)_5\text{Cl}]^{2+}$ , and DNA decreases the yield of guanine oxidation.<sup>24</sup> Our experiments required the use of  $[\text{Ru}(\text{NH}_3)_6]^{3+}$  as the quencher, since the reductive decomposition observed for the Co complex would prevent our ability to use repetitive photocycles. The DNA sequence we used is shown in Figure 5.5. This sequence encodes the *soxS* promoter, to which SoxR is known to bind specifically.<sup>65</sup> The remainder of the DNA strand provides ample room for the Ru oxidant to bind.

As with p53, the preparation of samples suitable for spectroscopic measurement proved challenging. At low protein concentrations, the protein is stable, but no signal can be observed. At high protein concentrations and following irradiation, precipitates tend to form. By systematically varying the buffer conditions, it was possible to find a buffer system that maintains protein stability at relatively high concentrations. This buffer included 50 mM sodium phosphate (pH 8) and 150 mM NaCl. At such high ionic strength, it is necessary to use 1 M  $[\text{Ru}(\text{NH}_3)_6]^{3+}$  to efficiently form the Ru(III) oxidant. Another challenge involves the requirement that SoxR remain in the reduced state. Since the presence of molecular oxygen in solution would lead to the oxidation of SoxR, precluding our ability to oxidize it using redox chemistry, the molecular oxygen scavenger dithionite must be included in solution. Samples must also be prepared anaerobically and sealed to prevent the introduction of oxygen.

### Dithionite Decreases Ru(II)\* Luminescence

The presence of dithionite has a strong effect on the kinetics of the system, even in the absence of SoxR. Without dithionite, a bleach is observed at 418 nm due to depletion of the Ru(II) ground state. This bleach exhibits a biexponential recovery with lifetimes of 61 ns (74%) and 1.1  $\mu\text{s}$  (26%) due to relaxation from the excited state and reaction of Ru(III), respectively. When 100  $\mu\text{M}$  dithionite is added, the intensity of the long-lived component increases and the recovery lifetimes change to 45 ns (55%) and 4.5  $\mu\text{s}$  (45%). When excess



### DNA Sequence

5'-GCG TTC GTA CGA GCT CTT TTC CAT AAA TCG CTT TAG GAG TTC AAT TGA ACT CCA ATT ATA CTC-3'  
 3'-CGC AAG CAT GCT CGA GAA AAG GTA TTT AGC GAA ATC CTC AAG TTA ACT TGA GGT TAA TAT GAG-5'

SoxR Binding Site

**Figure 5.5:** The SoxR transient absorption experiment. Top: Photoexcitation of  $[\text{Ru}(\text{phen})_2(\text{dppz})]^{2+}$  at 470 nm results in the formation of the ground state oxidant  $[\text{Ru}(\text{phen})_2(\text{dppz})]^{3+}$  following oxidative quenching by  $[\text{Ru}(\text{NH}_3)_6]^{3+}$  (Q). This Ru(III) species oxidizes guanine by DNA-mediated CT. Hole transfer from  $\text{G}^{\bullet+}$  to SoxR results in oxidation of the  $[\text{2Fe-2S}]$  cluster. Bottom: the DNA sequence used in SoxR oxidation experiments. The SoxR binding site is indicated.

dithionite is added, the intensity of the bleach decreases dramatically, and the fast recovery component is no longer observed. Similarly, in the absence of dithionite, Ru(II)\* emission at 610 nm decays with a rate of 52 ns. When dithionite is added, the intensity of emission decreases, although the emission lifetime remains approximately the same.

The TA and emission traces are shown in Figure 5.6. Of particular interest, the Stern-Volmer plot shows that the dependence of luminescence yield on dithionite concentration is linear. Since the lifetime of the emissive species does not change with increasing dithionite, it appears that Ru(II)\* luminescence is statically quenched by dithionite. Considering the low redox potential of dithionite (approximately  $-500$  mV vs. NHE),<sup>66</sup> it should easily be able to reduce the excited state of  $[\text{Ru}(\text{phen})_2(\text{dppz})]^{2+}$  ( $E^\circ[\text{Ru}^{2+*}/\text{Ru}^+] = 1.2$  V vs. NHE).<sup>67</sup> A static mechanism for this quenching is also reasonable since the electrostatic attraction between the Ru oxidant (2+) and dithionite (2-) should be quite strong.

If static quenching by dithionite occurs, then an additional reaction pathway from Ru(II)\* is possible. A revised reaction scheme is shown in Scheme 5.2. Notably, in the dithionite quenching experiments, the  $[\text{Ru}(\text{NH}_3)_6]^{3+}$  quencher was also present. In such systems, excitation to form Ru(II)\* can be followed by either oxidative quenching by  $[\text{Ru}(\text{NH}_3)_6]^{3+}$  or reductive quenching by dithionite. Dithionite could also presumably donate an electron to Ru(III), preventing the oxidation of guanine, or it could donate an electron to  $\text{G}^{\bullet+}$ , preventing the formation of permanent guanine damage as well as hole injection into SoxR.

### Preliminary Evidence for SoxR Oxidation

Comparison between oxidized SoxR and SoxR treated with dithionite under anaerobic conditions shows that oxidized SoxR absorbs more strongly than reduced SoxR between 380 nm and 580 nm.<sup>68</sup> Therefore, in transient absorption studies, we would expect to see an increase in the absorbance of the sample following photoexcitation and oxidation via the flash-quench technique.

Our best evidence for the DNA-mediated oxidation of SoxR was obtained using samples in which dithionite had been removed by dialysis in an anaerobic environment.

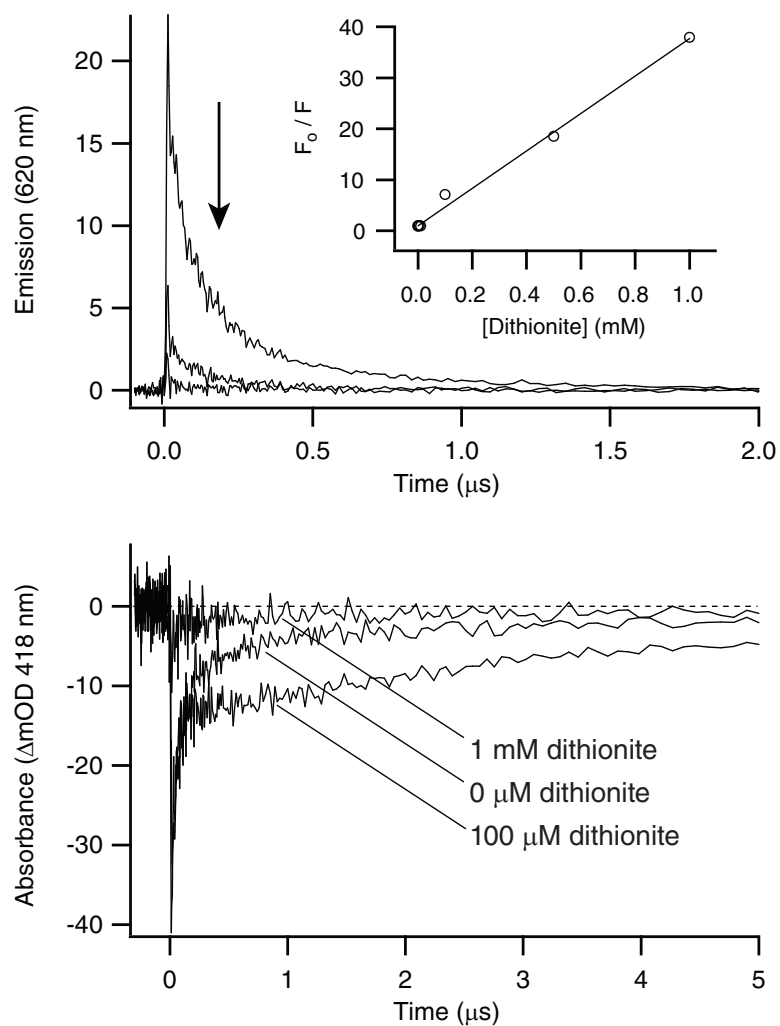


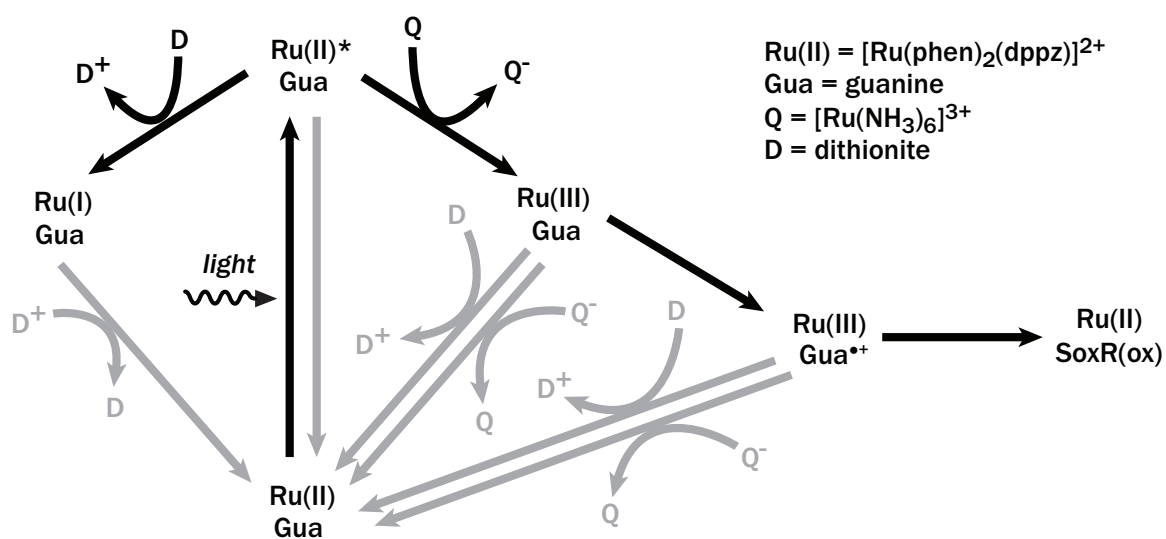
**Figure 5.6:** Transient absorption bleach recoveries at 418 nm and emission decay at 620 nm of 5  $\mu\text{M}$  DNA duplex, 10  $\mu\text{M}$   $[\text{Ru}(\text{phen})_2(\text{dppz})]^{2+}$ , 200  $\mu\text{M}$   $[\text{Ru}(\text{NH}_3)_6]^{3+}$ , and 0, 100, or 1000  $\mu\text{M}$  dithionite following 470 nm excitation. Inset: Stern-Volmer plot for the addition of dithionite ( $K = 3.67 \times 10^4 \text{ M}^{-1}$ ).

The protein was kept cold during dialysis in order to prevent cluster degradation. TA traces were measured at 418 nm for a sample consisting of 5  $\mu\text{M}$  DNA duplex, 10  $\mu\text{M}$   $[\text{Ru}(\text{phen})_2(\text{dppz})]^{2+}$ , 200  $\mu\text{M}$   $[\text{Ru}(\text{NH}_3)_6]^{3+}$ , and 5  $\mu\text{M}$  SoxR before and after introduction of ambient oxygen (Figure 5.7). In both traces, a large negative signal is seen at short times that recovers with a lifetime of 6.4  $\mu\text{s}$ . This bleach signal is due to the formation of Ru(III). In the reduced sample, a very weak, positive transient grows in with a lifetime of 20  $\mu\text{s}$  and persists for the duration of the measurement. After the introduction of ambient oxygen, this transient is no longer observed.

Although the intensity of the long-lifetime transient in the reduced sample is low, its appearance is consistent with the formation of oxidized SoxR as a result of DNA-mediated CT. While CT through DNA is expected to be very fast (10–100 ps),<sup>69</sup> CT through proteins will be much slower. The dependence of ET rate on distance has been determined in a wide variety of media.<sup>70</sup> Based on the crystal structure of oxidized SoxR bound to DNA,<sup>71</sup> the closest distance between the [2Fe-2S] cluster and the DNA base stack is 26 Å. From observations of ET through proteins, the time needed to transfer an electron over 26 Å should be approximately 1 ms. CT through SoxR is 50 $\times$  faster than this. At present, it is unclear whether the unexpectedly high CT rate is due to the presence of aromatic residues along the CT pathway, which have been shown to mediate ET in azurin.<sup>58</sup> It is also possible that the distance between the cluster and the DNA is shorter when the protein is in the reduced form (no crystal structure of reduced SoxR is available).

### 5.3.4 Endonuclease III

The BER glycosylase/lyase EndoIII is a redox-active protein involved with detecting and removing oxidized pyrimidines. All BER enzymes can be classified as either monofunctional DNA glycosylases, which remove damaged bases through insertion of an activated water molecule at the glycosidic bond, or glycosylase/lyases, which cleave the glycosidic bond via nucleophilic attack before degrading the associated sugar by Schiff base/conjugate elimination, leaving an apurinic/apyrimidinic (AP) site.<sup>72</sup> Some BER enzymes, such as the *E. coli* glycosylase/lyases MutY and EndoIII, contain  $[\text{4Fe-4S}]^{2+}$  clusters ligated by the sequence



**Scheme 5.2:** Flash-quench reduction and oxidation of  $\text{Ru(II)*}$ . Following photoexcitation,  $\text{Ru(II)}$  can be oxidized by  $[\text{Ru}(\text{NH}_3)_6]^{3+}$  or reduced by dithionite. Dithionite can also reduce  $\text{Ru(III)}$  and  $\text{G}^{\bullet+}$ , preventing the oxidation of SoxR.

Cys-X<sub>6</sub>-Cys-X<sub>2</sub>-Cys-X<sub>5</sub>-Cys.<sup>73</sup> This sequence is unique to cluster-bearing BER enzymes; the clusters of other proteins that contain iron-sulfur clusters, such as high-potential iron proteins (HiPIPs) and ferredoxins (Fds), possess different cluster ligation sequences.<sup>74</sup>

Although the general action of all BER enzymes is the same, the mechanisms by which they efficiently discover and distinguish between various oxidative lesions are poorly understood. Early mechanistic models suggested that the human glycosylase OGG1 recognizes its target lesion, 7,8-dihydro-8-oxo-2'-deoxyguanosine (8-oxo-dG), through specific hydrogen bonding interactions between the enzyme active site and 8-oxo-dG. However, this is only part of the picture; complexation of OGG1 with undamaged guanine results in only one fewer hydrogen bond than complexation with 8-oxo-dG. Such a subtle thermodynamic difference can hardly form the basis for accurate interrogation.<sup>75</sup> The mechanisms of recognition for more indiscriminate BER enzymes like EndoIII must be even more complex. The list of known substrates for EndoIII includes thymine glycol, cytosine glycol, urea, *N*-substituted urea, 5-hydroxy-5-methylhydantoin, and 5,6-dihydrothymine. Although these are all saturated, opened, or contracted pyrimidine rings, the broad spectrum of shapes and reactivity they present suggests that only careful study of the structure and dynamics of BER enzymes will lead to a full understanding of the mechanisms of lesion recognition.<sup>76</sup>

## Experimental Details

The focus of experiments involving EndoIII has been to measure the rate of CT to the protein cluster. Previously, the transient spectrum of an oxidized MutY/maltose binding protein fusion was observed using the flash-quench technique.<sup>29</sup> The transient spectrum of oxidized EndoIII is expected to exhibit a similar increase in absorbance near 410 nm, due to the greater molar extinction of the [4Fe-4S]<sup>3+</sup> cluster ( $\sim 20\,000\text{ M}^{-1}\text{ cm}^{-1}$ )<sup>77</sup> than the [4Fe-4S]<sup>2+</sup> cluster ( $17\,000\text{ M}^{-1}\text{ cm}^{-1}$ ).<sup>19</sup> In some experiments, the flash-quench technique was used in an effort to generate a high yield of oxidized protein. In other experiments, direct photooxidation was used so that the observable rates would not be limited by diffusion of the quencher (Figure 5.8). In these latter experiments, the oxidants [Rh(phi)<sub>2</sub>(bpy')]<sup>3+</sup>, [Ir(ppy)<sub>2</sub>(dppz')]<sup>+</sup>, and [Re(CO)<sub>3</sub>(dppz)(py')]<sup>+</sup> were used. Because these complexes bind

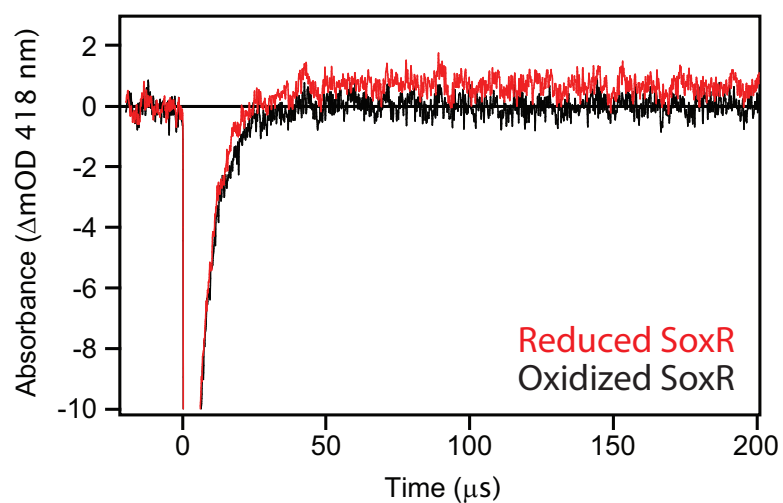


**Figure 5.7:** Transient absorption measured at 418 nm for samples of 5  $\mu M$  DNA duplex, 10  $\mu M$   $[Ru(phen)_2(dppz)]^{2+}$ , 200  $\mu M$   $[Ru(NH_3)_6]^{3+}$ , and 5  $\mu M$  SoxR. Before introduction of oxygen (red), a weak absorption is observed at long time. After introduction of oxygen (black), this component is no longer observed.

to DNA through different ligands and show different oxidation efficiencies,<sup>78</sup> we expected that one of them would be a better redox partner with EndoIII than the other two. All three complexes can be covalently linked to DNA through carboxyalkyl linkers, ensuring a 1:1 ratio of complex to DNA.

### Experiments Using the Flash-Quench Technique

Early experiments with EndoIII involved an analogous system to that used by Yavin et al. for the oxidation of MutY. One equivalent of EndoIII was included in solution with 20  $\mu\text{M}$   $[\text{Ru}(\text{phen})_2(\text{dppz})]^{2+}$ , 600  $\mu\text{M}$   $[\text{Ru}(\text{NH}_3)_6]^{3+}$ , and excess poly(dG-dC). Excitation at 470 nm led to oxidation of guanine by the flash-quench technique. The  $\text{G}^{\bullet+}$  species formed should be sufficiently oxidizing to oxidize the  $[\text{4Fe-4S}]^{2+}$  cluster of the protein. The results of the experiment are shown in Figure 5.9. In the absence of quencher and EndoIII, a short lived bleach appears with recovery lifetimes of 41 ns (62%) and 320 ns (38%). This bleach is due to formation of the  $\text{Ru}(\text{II})^*$  excited state. With the addition of quencher, the bleach recovery lifetime shortens to 34 ns, and a transient appears that decays with a lifetime of 21  $\mu\text{s}$ . Based on similar observations in a nearly identical system, this transient can be assigned to the neutral guanine radical,  $\text{G}^\bullet$ .<sup>27</sup> When EndoIII is added, interestingly, the lifetime of the short-lived component is similar to that observed without protein, but the guanine radical no longer appears. Instead, a negative signal with a large amplitude is observed. The recovery lifetime of this component is 6.1  $\mu\text{s}$ .

According to our reaction model, a new transient is expected when EndoIII is added. However, based on comparisons between the absorption spectra of the 2+ and 3+ states of other  $[\text{4Fe-4S}]$  proteins such as Fds and HiPIPs, the transient formed upon oxidation of EndoIII should give a positive signal, not a negative one. The identity of the species that generates this large negative signal is therefore difficult to determine. In control samples lacking an oxidant, no signal was observed. The only transient species that are expected to cause a decrease in the absorbance at 410 nm are the degraded  $[\text{4Fe-4S}]^+$  cluster,  $\text{Ru}(\text{II})^*$  and  $\text{Ru}(\text{III})$ . If the cluster is being degraded, a permanent decrease in absorption should be observed; here, the signal recovers to the baseline over time. It is very unlikely that

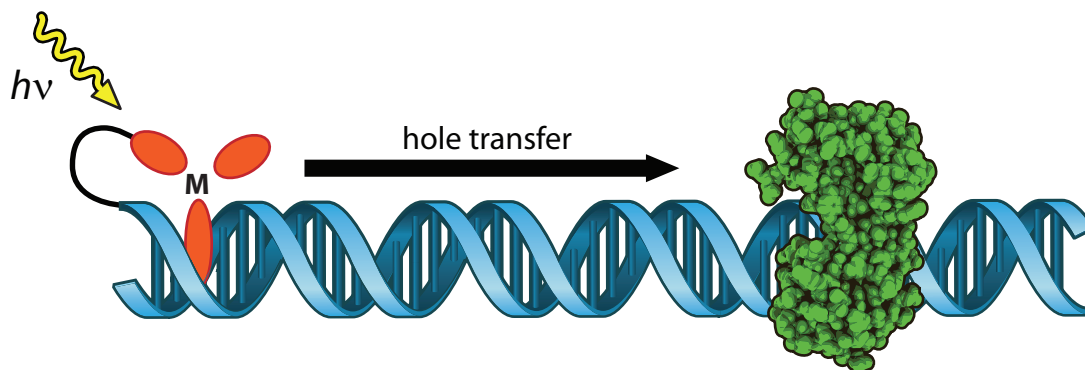
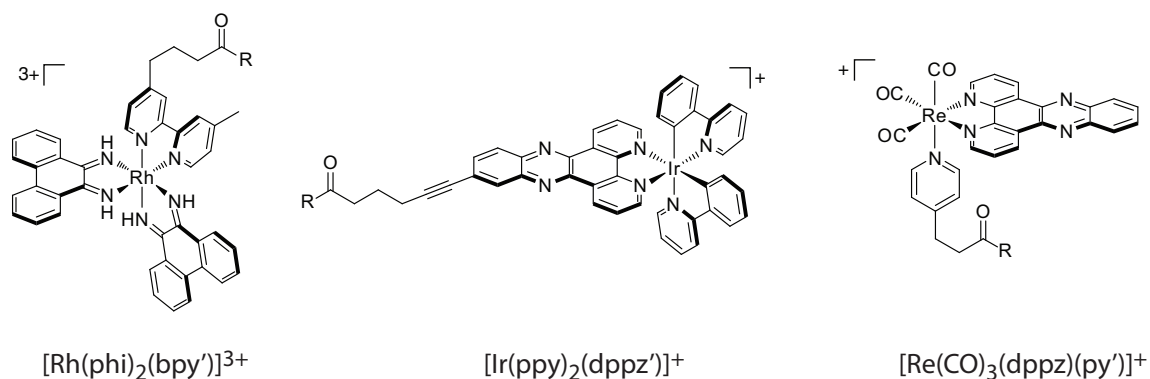


**Figure 5.8:** The EndoIII transient absorption experiment. Top: structures of the intercalating photooxidants  $[\text{Rh}(\text{phi})_2(\text{bpy}') ]^{3+}$ ,  $[\text{Ir}(\text{ppy})_2(\text{dppz}') ]^{+}$ , and  $[\text{Re}(\text{CO})_3(\text{dppz})(\text{py}') ]^{+}$  and metal complex-DNA conjugates. Bottom: excitation of the covalent photooxidant results in charge injection, forming the guanine cation radical,  $\text{G}^{\bullet+}$ . Hole transfer to EndoIII results in oxidation of the  $[\text{4Fe-4S}]^{2+}$  cluster to form  $[\text{4Fe-4S}]^{3+}$ .

the addition of EndoIII results in an increase in the excited state lifetime of Ru(II) by over two orders of magnitude. However, the other alternative, that addition of protein results in a longer-lived Ru(III) species is also difficult to reconcile considering the high guanine content still present and the facile oxidation of guanine observed in the absence of protein. Another interpretation involves formation of the reduced cluster. The one-electron reduced  $[4\text{Fe-4S}]^+$  cluster is expected to absorb 10–20% less at 410 nm than the  $[4\text{Fe-4S}]^{2+}$  cluster.<sup>19</sup> If the signal is due to reduced EndoIII, the identity of the reductant is unclear. Solution studies indicate that the reduction potential of EndoIII in solution is  $< -600$  mV vs. NHE,<sup>79</sup> and electrochemistry experiments on graphite surfaces suggest that it is closer to  $-300$  mV.<sup>9</sup> The reduction potential of EndoIII bound to DNA could not be determined electrochemically, suggesting that it is outside the operating range of the electrochemical instrument ( $E^\circ < -300$  mV). In any case, the reduced quencher,  $[\text{Ru}(\text{NH}_3)_6]^{2+}$  is not sufficiently strong to reduce the protein ( $E^\circ[\text{Ru}^{3+}/\text{Ru}^{2+}] = 50$  mV vs. NHE).<sup>80</sup> The oxidation potential of  $[\text{Ru}(\text{phen})_2(\text{dppz})]^{2+*}$  is  $-0.72$  V vs. NHE,<sup>81</sup> indicating that excited Ru may be strong enough to reduce EndoIII. Such a pathway, however, would have to compete with oxidative quenching. This seems unlikely considering the much higher concentration and much more facile diffusion of  $[\text{Ru}(\text{NH}_3)_6]^{3+}$  than of EndoIII.

Additional control experiments will be necessary before the behavior of this flash-quench system can be fully understood. For example, the ability of EndoIII to quench the Ru(II)\* excited state could be tested by observing the dependence of Ru(II)\* luminescence lifetime and yield on EndoIII concentration. Measurement of transient spectra at various delay times after laser excitation may also provide information about the particular species present in solution throughout the reaction.

### Direct Photooxidation Experiments

In order to remove complications introduced by the diffusing quencher on the EndoIII oxidation pathway, several systems were studied involving direct photooxidants rather than the flash-quench technique. Figure 5.10 shows transient spectra of  $15 \mu\text{M}$  Ir-DNA, Rh-DNA, and Re-DNA conjugates in the absence and presence of  $15 \mu\text{M}$  EndoIII at 60 ns following

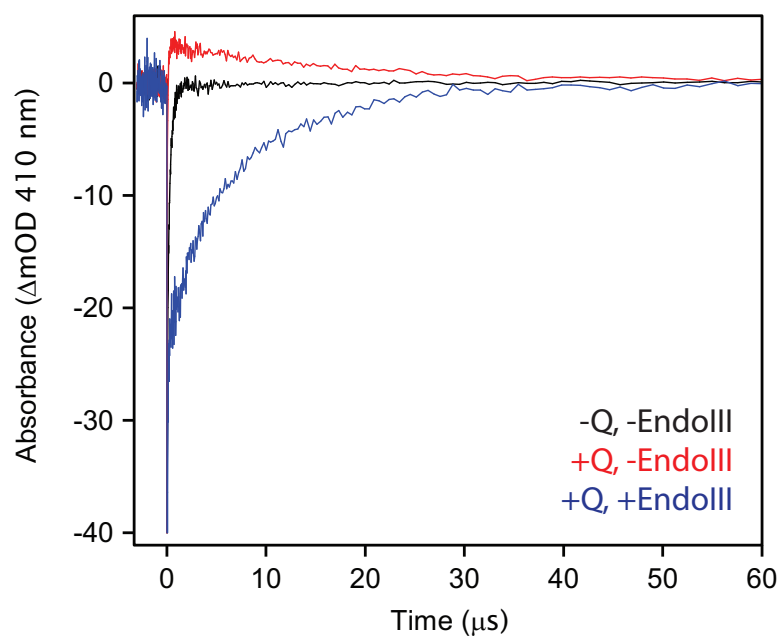


**Figure 5.9:** Transient absorption of  $20 \mu\text{M}$   $[\text{Ru}(\text{phen})_2(\text{dppz})]^{2+}$  in the presence of  $1 \text{ mM}$  (base pairs) poly(dG-dC),  $600 \mu\text{M}$   $[\text{Ru}(\text{NH}_3)_6]^{2+}$  quencher, and  $20 \mu\text{M}$  EndoIII in buffer ( $10 \text{ mM}$   $\text{NaP}_i$ ,  $50 \text{ mM}$   $\text{NaCl}$ ;  $\text{pH}$   $7.5$ ). In the absence of quencher and EndoIII (black), no long-lived products are formed. In the presence of quencher (red), a long-lived positive transient is observed. With both quencher and EndoIII (blue) a long-lived negative signal appears.

355 nm photoexcitation. Interestingly, the three systems behave quite differently. In the Ir system, the introduction of EndoIII results in a decrease in absorption in the bleach region (between 390 nm and 425 nm) and an increase in the absorption at higher wavelengths. Thus, it appears that no new absorbing species are formed, but that the intensity of the Ir transient increases. In the Rh system, the opposite is true. No new absorbing species are observed, but the intensity of the Rh signal decreases with the addition of protein. In the Re system, no change is observed upon the introduction of EndoIII.

Based on comparisons between the reduced state spectra of the metal complexes determined by spectroelectrochemistry and the transient absorption spectra of the metal complex-DNA conjugates obtained by transient absorption spectroscopy, it appears that the transient signals seen in the absence of EndoIII are due to the formation of the reduced metal complexes, or to mixtures of excited and reduced states.<sup>78</sup> This interpretation is consistent with the excited state redox properties of the complexes; each of them should be sufficiently strong excited state oxidants to form  $G^{\bullet+}$ , resulting in reduction of the complexes themselves. Comparing these results with spectra obtained in the absence and presence of EndoIII, then, suggests that the addition of protein increases the concentration of the reduced Ir species and decreases the concentration of the reduced Rh species, while the Re conjugate is unaffected. The increase in the concentration of reduced Ir upon the addition of EndoIII is consistent with our reaction model, since the addition of protein provides an additional low potential hole trap and decreases the propensity for BET. The decrease in the concentration of reduced Rh with the addition of EndoIII, however, is difficult to explain. It does not appear that EndoIII interacts with the excited state of Rh, since the lifetime of the signal is  $\sim 150$  ns with and without protein. Inner filtering by the protein can be ruled out, since a similar effect would be observed in the Ir sample as well. The lack of change in the Re sample can be explained by inefficient hole injection, since other studies suggest that a large population of  $Re^*$  persists after excitation, even in the presence of DNA containing guanine.<sup>78,82</sup>

Interestingly, titrations with EndoIII show that the intensity of the negative TA signal near 400 nm in Ir-DNA samples depends directly on the concentration of protein in

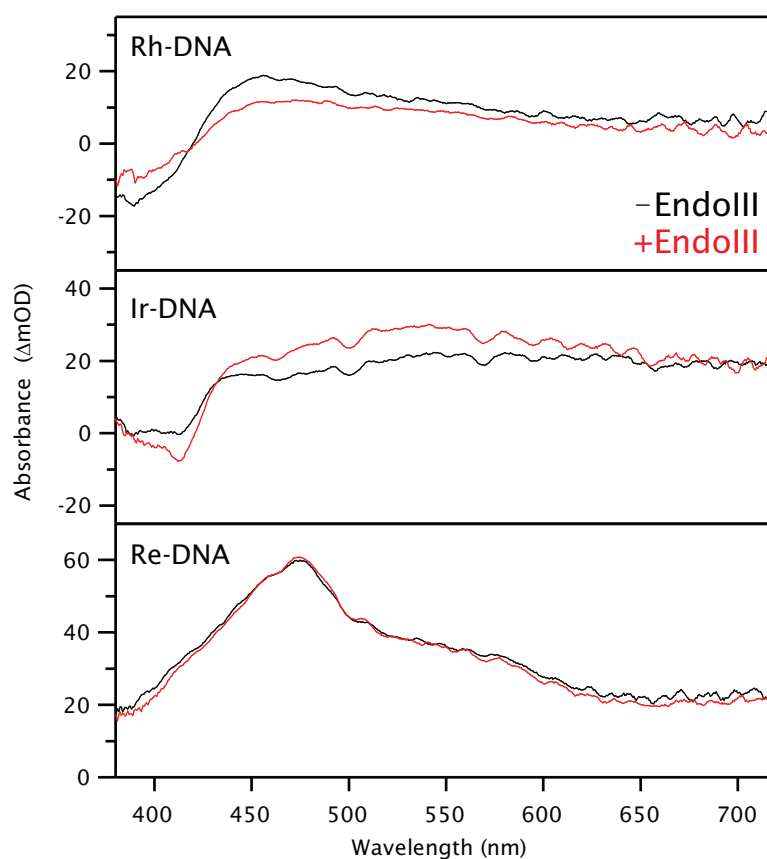


**Figure 5.10:** Transient absorption spectra of metal complex-DNA conjugates with and without EndoIII. The metal complexes  $[\text{Rh}(\text{phi})_2(\text{bpy}')^{3+}$ ,  $[\text{Ir}(\text{ppy})_2(\text{dppz}')^+]$ , and  $[\text{Re}(\text{CO})_3(\text{dppz})(\text{py}')^+]$  were covalently tethered to the 5'-ends of DNA strands with the sequence 5'-ACAITATACCGACTGACTGACT-3'. The transient absorption spectra of the associated DNA duplexes ( $20 \mu\text{M}$ ) were recorded 60 ns after 355 nm photoexcitation in the absence (black) and presence (red) of  $20 \mu\text{M}$  EndoIII.

solution (Figure 5.11). No change in lifetime is observed, however. Similarly, the intensity of the positive transient near 450 nm increases increasing EndoIII concentration, and the lifetime of the transient decreases from 240 ns with 0 equivalents of EndoIII to 190 ns with 4 equivalents.

The changes observed in the TA spectra and kinetics traces of metal complex-DNA conjugates upon the addition of EndoIII indicate that some physical or chemical change is occurring. We expect that oxidation of the protein cluster should occur; however, no direct evidence has been observed for such a process. Instead, data suggest that changes in the lifetimes and intensities of the observed transients are due to changes in the efficiency of metal complex reduction or BET. These results, therefore, may comprise secondary evidence for DNA-mediated EndoIII oxidation. Evidence for photochemistry can also be observed in steady-state spectrophotometric measurements made before and after photolysis. In the absence of protein, little change is observed in the spectra. In the presence of protein, large differences are typically observed, including a decrease in the absorption of the  $[4\text{Fe-4S}]^{2+}$  cluster and increased absorbance at higher wavelengths. Such differences are consistent with degradative oxidation of the cluster.

## 5.4 Concluding Remarks

Experiments in a variety of systems show that DNA-mediated CT is possible in a biological context. The efficiency of CT can be modulated by protein binding, and evidence is accumulating for the specific utilization of DNA-mediated oxidation in cellular processes such as damage sequestration, lesion detection, and transcriptional activation. Transient absorption experiments involving several redox-active DNA-binding proteins have provided initial direct evidence for similar processes *in vitro*. Oxidation of p53 by the flash-quench technique leads to the formation of a small transient band that bears the signatures of the tyrosine radical cation. Oxidation of SoxR by the flash-quench technique after removal of dithionite has similarly provided tantalizing evidence for the oxidation of the protein by DNA-mediated CT. Finally, experiments with EndoIII involving DNA-conjugated intercalating metal complex photooxidants show that the presence of the protein perturbs the

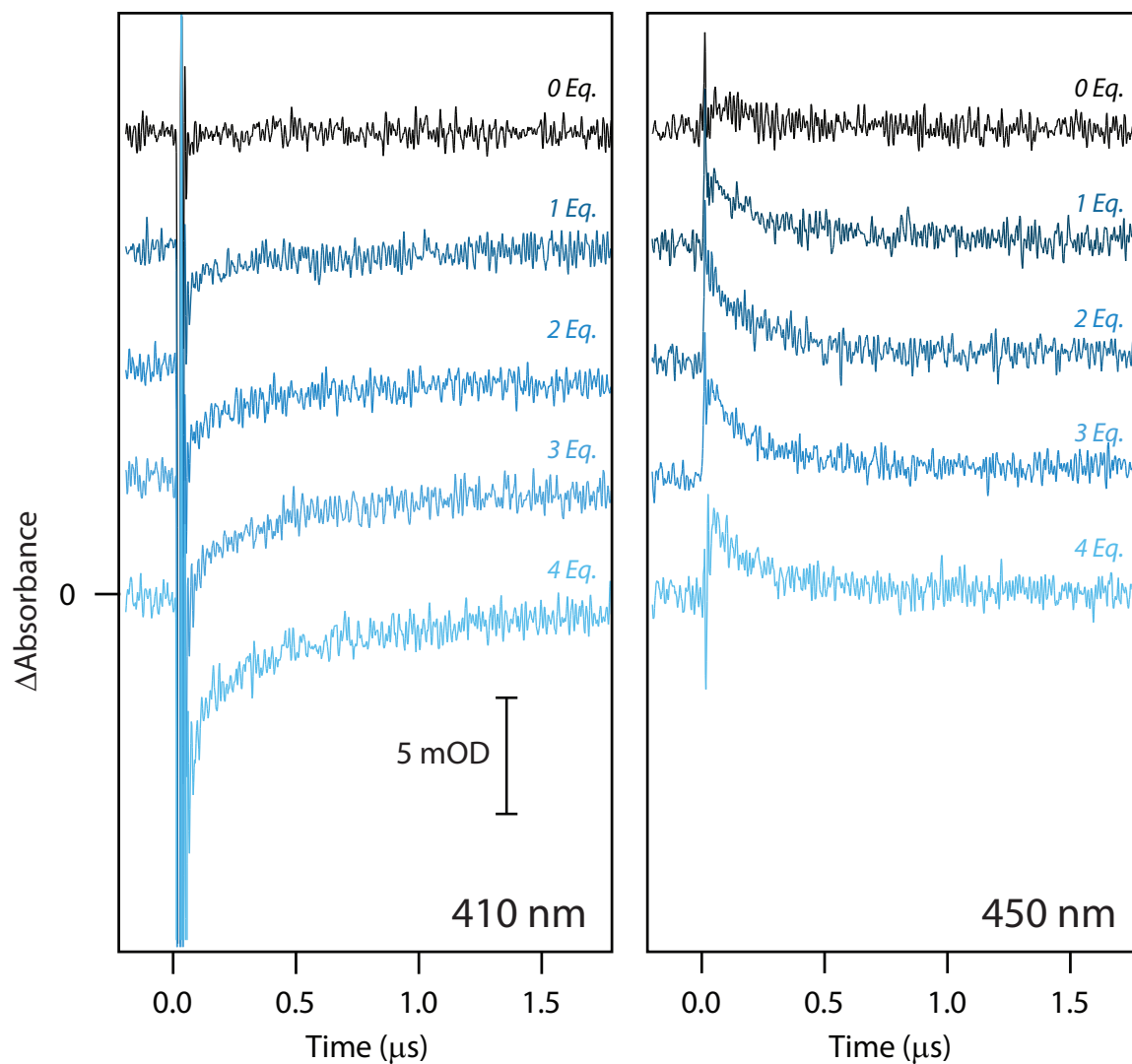


**Figure 5.11:** Transient absorption spectra of 5  $\mu$ M Ir-DNA with increasing amounts of EndoIII (0, 1, 2, 3, or 4 equivalents, as indicated). Kinetics were measured at 410 nm (left) and 450 nm (right). Samples were excited at 355 nm. Traces are vertically offset for clarity.

system, although further experiments are needed to fully understand the processes that are occurring. In all of the systems described here, expanded exploration of the experimental parameters is expected to increase the quality of the data, leading to more consistent explanations for the chemistry that is occurring and a greater understanding of the role that redox-active proteins may play in DNA-mediated CT. This work therefore provides a solid basis for future experiments.

## References

- [1] Genereux, J. C., and Barton, J. K. "Mechanisms for DNA charge transport." *Chem. Rev.* **110**, 1642–1662 (2010).
- [2] Kelley, S. O., Boon, E. M., Barton, J. K., Jackson, N. M., and Hill, M. G. "Single-base mismatch detection based on charge transduction through DNA." *Nucl. Acids Res.* **27**, 4830–4837 (1999).
- [3] Boon, E. M., Ceres, D. M., Drummond, T. G., Hill, M. G., and Barton, J. K. "Mutation detection by electrocatalysis at DNA-modified electrodes." *Nat. Biotech.* **18**, 1096–1100 (2000).
- [4] Boal, A. K., and Barton, J. K. "Electrochemical detection of lesions in DNA." *Bioconj. Chem.* **16**, 312–321 (2005).
- [5] Rajski, S. R., Kumar, S., Roberts, R. J., and Barton, J. K. "Protein-Modulated DNA Electron Transfer." *J. Am. Chem. Soc.* **121**, 5615–5616 (1999).
- [6] Rajski, S. R., and Barton, J. K. "How different DNA-binding proteins affect long-range oxidative damage to DNA." *Biochemistry* **40**, 5556–5564 (2001).
- [7] Boon, E. M., Salas, J. E., and Barton, J. K. "An electrical probe of protein-DNA interactions on DNA-modified surfaces." *Nat. Biotech.* **20**, 282–286 (2002).
- [8] Gorodetsky, A. A., Hammond, W. J., Hill, M. G., Slowinski, K., and Barton, J. K. "Scanning electrochemical microscopy of DNA monolayers modified with Nile Blue." *Langmuir* **24**, 14282–14288 (2008).
- [9] Gorodetsky, A. A., Ebrahim, A., and Barton, J. K. "Electrical detection of TATA binding protein at DNA-modified microelectrodes." *J. Am. Chem. Soc.* **130**, 2924–2925 (2008).
- [10] Wagenknecht, H.-A., Rajski, S. R., Pascaly, M., Stemp, E. D. A., and Barton, J. K. "Direct observation of radical intermediates in protein-dependent DNA charge transport." *J. Am. Chem. Soc.* **123**, 4400–4407 (2001).

- [11] Núñez, M. E., Noyes, K. T., and Barton, J. K. "Oxidative charge transport through DNA in nucleosome core particles." *Chem. Biol.* **9**, 403–415 (2002).
- [12] Núñez, M. E., Holmquist, G. P., and Barton, J. K. "Evidence for DNA Charge Transport in the Nucleus." *Biochemistry* **40**, 12465–12471 (2001).
- [13] Merino, E. J., and Barton, J. K. "Oxidation by DNA charge transport damages conserved sequence block II, a regulatory element in mitochondrial DNA." *Biochemistry* **46**, 2805–2811 (2007).
- [14] Merino, E. J., and Barton, J. K. "DNA oxidation by charge transport in mitochondria." *Biochemistry* **47**, 1511–1517 (2008).
- [15] Merino, E. J., Davis, M. L., and Barton, J. K. "Common mitochondrial DNA mutations generated through DNA-mediated charge transport." *Biochemistry* **48**, 660–666 (2009).
- [16] Wagenknecht, H.-A., Stemp, E. D. A., and Barton, J. K. "DNA-Bound peptide radicals generated through DNA-mediated electron transport." *Biochemistry* **39**, 5483–5491 (2000).
- [17] Wagenknecht, H.-A., Stemp, E. D. A., and Barton, J. K. "Evidence of Electron Transfer from Peptides to DNA: Oxidation of DNA-Bound Tryptophan Using the Flash-Quench Technique." *J. Am. Chem. Soc.* **122**, 1–7 (2000).
- [18] Augustyn, K. E., Merino, E. J., and Barton, J. K. "A role for DNA-mediated charge transport in regulating p53: Oxidation of the DNA-bound protein from a distance." *Proc. Natl. Acad. Sci. USA* **104**, 18907–18912 (2007).
- [19] Cunningham, R. P., Asahara, H., Bank, J. F., Scholes, C. P., Salerno, J. C., Surerus, K., Munck, E., McCracken, J., Peisach, J., and Emptage, M. H. "Endonuclease III is an iron-sulfur protein." *Biochemistry* **28**, 4450–4455 (1989).
- [20] Gorodetsky, A. A., Boal, A. K., and Barton, J. K. "Direct electrochemistry of endonuclease III in the presence and absence of DNA." *J. Am. Chem. Soc.* **128**, 12082–12083 (2006).

- [21] Boal, A. K., Yavin, E., Lukianova, O. A., O'Shea, V. L., David, S. S., and Barton, J. K. "DNA-bound redox activity of DNA repair glycosylases containing [4Fe-4S] clusters." *Biochemistry* **44**, 8397–8407 (2005).
- [22] Boon, E. M., Livingston, A. L., Chmiel, N. H., David, S. S., and Barton, J. K. "DNA-mediated charge transport for DNA repair." *Proc. Natl. Acad. Sci. USA* **100**, 12543–12547 (2003).
- [23] Gorodetsky, A. A., Dietrich, L. E. P., Lee, P. E., Demple, B., Newman, D. K., and Barton, J. K. "DNA binding shifts the redox potential of the transcription factor SoxR." *Proc. Natl. Acad. Sci. USA* **105**, 3684–3689 (2008).
- [24] Lee, P. E., Demple, B., and Barton, J. K. "DNA-mediated redox signaling for transcriptional activation of SoxR." *Proc. Natl. Acad. Sci. USA* **106**, 13164–13168 (2009).
- [25] Núñez, M. E., Hall, D. B., and Barton, J. K. "Long-range oxidative damage to DNA: effects of distance and sequence." *Chem. Biol.* **6**, 85–97 (1999).
- [26] Boal, A. K., Genereux, J. C., Sontz, P. A., Gralnick, J. A., Newman, D. K., and Barton, J. K. "Redox signaling between DNA repair proteins for efficient lesion detection." *Proc. Natl. Acad. Sci. USA* **106**, 15237–15242 (2009).
- [27] Stemp, E. D. A., Arkin, M. R., and Barton, J. K. "Oxidation of Guanine in DNA by  $\text{Ru}(\text{phen})_2(\text{dppz})^{3+}$  Using the Flash-Quench Technique." *J. Am. Chem. Soc.* **119**, 2921–2925 (1997).
- [28] Stemp, E. D. A., and Barton, J. K. "The Flash-Quench Technique in Protein-DNA Electron Transfer: Reduction of the Guanine radical by Ferrocycytochrome *c*." *Inorg. Chem.* **39**, 3868–3874 (2000).
- [29] Yavin, E., Boal, A. K., Stemp, E. D. A., Boon, E. M., Livingston, A. L., O'Shea, V. L., David, S. S., and Barton, J. K. "Protein-DNA charge transport: redox activation of a DNA repair protein by guanine radical." *Proc. Natl. Acad. Sci. USA* **102**, 3546–3551 (2005).

- [30] Shao, F., Elias, B., Lu, W., and Barton, J. K. "Synthesis and characterization of iridium(III) cyclometalated complexes with oligonucleotides: insights into redox reactions with DNA." *Inorg. Chem.* **46**, 10187–10199 (2007).
- [31] Sitlani, A., Long, E. C., Pyle, A. M., and Barton, J. K. "DNA Photocleavage by Phenanthrenequinone Diimine Complexes of Rhodium(III): Shape-Selective Recognition and Reaction." *J. Am. Chem. Soc.* **114**, 2303–2312 (1992).
- [32] Boal, A. K. "DNA-Mediated Charge Transport in DNA Repair." Ph.D. thesis, California Institute of Technology, 2008.
- [33] Dempsey, J. L., Winkler, J. R., and Gray, H. B. "Kinetics of electron transfer reactions of H<sub>2</sub>-evolving cobalt diglyoxime catalysts." *J. Am. Chem. Soc.* **132**, 1060–1065 (2010).
- [34] Shao, F., Augustyn, K. E., and Barton, J. K. "Sequence dependence of charge transport through DNA domains." *J. Am. Chem. Soc.* **127**, 17445–17452 (2005).
- [35] Hall, D. B., and Barton, J. K. "Sensitivity of DNA-Mediated Electron Transfer to the Intervening  $\pi$ -Stack: A Probe for the Integrity of the DNA Base Stack." *J. Am. Chem. Soc.* **119**, 5045–5046 (1997).
- [36] Odom, D. T., Dill, E. A., and Barton, J. K. "Robust charge transport in DNA double crossover assemblies." *Chem. Biol.* **7**, 475–481 (2000).
- [37] Odom, D. T., Dill, E. a., and Barton, J. K. "Charge transport through DNA four-way junctions." *Nucl. Acids Res.* **29**, 2026–2033 (2001).
- [38] Delaney, S., and Barton, J. K. "Charge transport in DNA duplex/quadruplex conjugates." *Biochemistry* **42**, 14159–14165 (2003).
- [39] Williams, T. T., Odom, D. T., and Barton, J. K. "Variations in DNA Charge Transport with Nucleotide Composition and Sequence." *J. Am. Chem. Soc.* **122**, 9048–9049 (2000).

- [40] Boon, E. M., Pope, M. A., Williams, S. D., David, S. S., and Barton, J. K. "DNA-Mediated Charge Transport as a Probe of MutY/DNA Interaction." *Biochemistry* **41**, 8464–8470 (2002).
- [41] Dandliker, P. J., Holmlin, R. E., and Barton, J. K. "Oxidative Thymine Dimer Repair in the DNA Helix." *Science* **275**, 1465–1468 (1997).
- [42] Dandliker, P. J., Núñez, M. E., and Barton, J. K. "Oxidative charge transfer To repair thymine dimers and damage guanine bases in DNA assemblies containing tethered metallointercalators." *Biochemistry* **37**, 6491–6502 (1998).
- [43] Shao, F., and Barton, J. K. "Long-range electron and hole transport through DNA with tethered cyclometalated iridium(III) complexes." *J. Am. Chem. Soc.* **129**, 14733–14738 (2007).
- [44] Elias, B., Shao, F., and Barton, J. K. "Charge migration along the DNA duplex: hole versus electron transport." *J. Am. Chem. Soc.* **130**, 1152–1153 (2008).
- [45] Elias, B., Genereux, J. C., and Barton, J. K. "Ping-pong electron transfer through DNA." *Angew. Chem. Int. Ed.* **47**, 9067–9070 (2008).
- [46] Arkin, M. R., Stemp, E. D. A., Coates Pulver, S., and Barton, J. K. "Long-range oxidation of guanine by Ru(III) in duplex DNA." *Chem. Biol.* **4**, 389–400 (1997).
- [47] Schiemann, O., Turro, N. J., and Barton, J. K. "EPR Detection of Guanine Radicals in a DNA Duplex under Biological Conditions: Selective Base Oxidation by Ru(phen)<sub>2</sub>dppz<sup>3+</sup> Using the Flash-Quench Technique." *J. Phys. Chem. B* **104**, 7214–7220 (2000).
- [48] Bhattacharya, P. K., and Barton, J. K. "Influence of intervening mismatches on long-range guanine oxidation in DNA duplexes." *J. Am. Chem. Soc.* **123**, 8649–8656 (2001).
- [49] Delaney, S., Yoo, J., Stemp, E. D. A., and Barton, J. K. "Charge equilibration between two distinct sites in double helical DNA." *Proc. Natl. Acad. Sci. USA* **101**, 10511–10516 (2004).

- [50] Yoo, J., Delaney, S., Stemp, E. D. A., and Barton, J. K. "Rapid radical formation by DNA charge transport through sequences lacking intervening guanines." *J. Am. Chem. Soc.* **125**, 6640–6641 (2003).
- [51] Pascaly, M., Yoo, J., and Barton, J. K. "DNA mediated charge transport: characterization of a DNA radical localized at an artificial nucleic acid base." *J. Am. Chem. Soc.* **124**, 9083–9092 (2002).
- [52] Copeland, K. D., Lueras, A. M. K., Stemp, E. D. A., and Barton, J. K. "DNA cross-linking with metallointercalator-peptide conjugates." *Biochemistry* **41**, 12785–12797 (2002).
- [53] Vousden, K. H., and Lu, X. "Live or let die: the cell's response to p53." *Nat. Rev. Cancer* **2**, 594–604 (2002).
- [54] Ang, H. C., Joerger, A. C., Mayer, S., and Fersht, A. R. "Effects of common cancer mutations on stability and DNA binding of full-length p53 compared with isolated core domains." *J. Biol. Chem.* **281**, 21934–21941 (2006).
- [55] Joerger, A. C., and Fersht, A. R. "Structure-function-rescue: the diverse nature of common p53 cancer mutants." *Oncogene* **26**, 2226–2242 (2007).
- [56] El-Deiry, W. S., Kern, S. E., Pietenpol, J. A., Kinzler, K. W., and Vogelstein, B. "Definition of a consensus binding site for p53." *Nat. Genet.* **1**, 45–49 (1992).
- [57] Nikolova, P. V., Henckel, J., Lane, D. P., and Fersht, A. R. "Semirational design of active tumor suppressor p53 DNA binding domain with enhanced stability." *Proc. Natl. Acad. Sci. USA* **95**, 14675–14680 (1998).
- [58] Shih, C., Museth, A. K., Abrahamsson, M., Blanco-Rodríguez, A. M., Di Bilio, A. J., Sudhamsu, J., Crane, B. R., Ronayne, K. L., Towrie, M., Vlček, A., Richards, J. H., Winkler, J. R., and Gray, H. B. "Tryptophan-accelerated electron flow through proteins." *Science* **320**, 1760–1762 (2008).
- [59] Williams, J. W., and Drissen, E. M. "Oxidation-Reduction Potentials of Certain Sulfhydryl Compounds." *J. Biol. Chem.* **87**, 441–451 (1930).

- [60] Murphy, C. J., Arkin, M. R., Ghatlia, N. D., Bossmann, S. H., Turro, N. J., and Barton, J. K. "Fast photoinduced electron transfer through DNA intercalation." *Proc. Natl. Acad. Sci. USA* **91**, 5315–5319 (1994).
- [61] Steenken, S., and Jovanovic, S. V. "How Easily Oxidizable Is DNA? One-Electron Reduction Potentials of Adenosine and Guanosine Radicals in Aqueous Solution." *J. Am. Chem. Soc.* **119**, 617–618 (1997).
- [62] Romano, C. A., Sontz, P. A., and Barton, J. K. "Mutants of the Base Excision Repair Glycosylase, Endonuclease III: DNA Charge Transport as a First Step in Lesion Detection." *Biochemistry* **50**, 6133–6145 (2011).
- [63] Hidalgo, E., and Demple, B. "An iron-sulfur center essential for transcriptional activation by the redox-sensing SoxR protein." *EMBO J.* **13**, 138–146 (1994).
- [64] Ding, H., Hidalgo, E., and Demple, B. "The redox state of the [2Fe-2S] clusters in SoxR protein regulates its activity as a transcription factor." *J. Biol. Chem.* **271**, 33173–33175 (1996).
- [65] Hidalgo, E., Leautaud, V., and Demple, B. "The redox-regulated SoxR protein acts from a single DNA site as a repressor and an allosteric activator." *EMBO J.* **17**, 2629–2636 (1998).
- [66] Mayhew, S. G. "The Redox Potential of Dithionite and  $\text{SO}_2^-$  from Equilibrium Reactions with Flavodoxins, Methyl Viologen and Hydrogen plus Hydrogenase." *Eur. J. Biochem.* **85**, 535–547 (1978).
- [67] Moucheron, C., Kirsch-De Mesmaeker, A., and Choua, S. "Photophysics of  $\text{Ru}(\text{phen})_2(\text{PHEHAT})^{2+}$ : A Novel 'Light Switch' for DNA and Photo-oxidant for Mononucleotides." *Inorg. Chem.* **36**, 584–592 (1997).
- [68] Hidalgo, E., Bollinger, J. M., Bradley, T. M., Walsh, C. T., and Demple, B. "Binuclear [2Fe-2S] clusters in the Escherichia coli SoxR protein and role of the metal centers in transcription." *J. Biol. Chem.* **270**, 20908–20914 (1995).

- [69] Wan, C., Fiebig, T., Kelley, S. O., Treadway, C. R., Barton, J. K., and Zewail, A. H. “Femtosecond dynamics of DNA-mediated electron transfer.” *Proc. Natl. Acad. Sci. USA* **96**, 6014–6019 (1999).
- [70] Tezcan, F. A., Crane, B. R., Winkler, J. R., and Gray, H. B. “Electron tunneling in protein crystals.” *Proc. Natl. Acad. Sci. USA* **98**, 5002–5006 (2001).
- [71] Watanabe, S., Kita, A., Kobayashi, K., and Miki, K. “Crystal structure of the [2Fe-2S] oxidative-stress sensor SoxR bound to DNA.” *Proc. Natl. Acad. Sci. USA* **105**, 4121–4126 (2008).
- [72] Verdine, G. L., and Bruner, S. D. “How do DNA repair proteins locate damaged bases in the genome?” *Chem. Biol.* **4**, 329–334 (1997).
- [73] Thayer, M. M., Ahern, H., Xing, D., Cunningham, R. P., and Tainer, J. A. “Novel DNA binding motifs in the DNA repair enzyme endonuclease III crystal structure.” *EMBO J.* **14**, 4108–4120 (1995).
- [74] Kuo, C.-F., Mcrec, D. E., Fisher, C. L., O’Handley, S. F., Cunningham, R. P., and Tainer, J. A. “Atomic Structure of the DNA Repair [4Fe-4S] Enzyme Endonuclease III.” *Science* **258**, 434–440 (1992).
- [75] van Loon, B., Markkanen, E., and Hübscher, U. “Oxygen as a friend and enemy: How to combat the mutational potential of 8-oxo-guanine.” *DNA repair* **9**, 604–616 (2010).
- [76] Aspinwall, R., Rothwell, D. G., Roldan-Arjona, T., Anselmino, C., Ward, C. J., Cheadle, J. P., Sampson, J. R., Lindahl, T., Harris, P. C., and Hickson, I. D. “Cloning and characterization of a functional human homolog of Escherichia coli endonuclease III.” *Proc. Natl. Acad. Sci. USA* **94**, 109–114 (1997).
- [77] Lippard, S. J., and Berg, J. M. *Principles of Bioinorganic Chemistry*; University Science Books: Mill Valley, California, 1994.
- [78] Olmon, E. D., Hill, M. G., and Barton, J. K. “Using Metal Complex Reduced States to Monitor the Oxidation of DNA.” *Inorg. Chem.* **Submitted**, (2011).

- [79] Fu, W., O’Handley, S., Cunningham, R. P., and Johnson, M. K. “The Role of the Iron-Sulfur Cluster in *Escherichia coli* Endonuclease III: A Resonance Raman Study.” *J. Biol. Chem.* **267**, 16135–16137 (1992).
- [80] Stemp, E. D. A., Holmlin, R. E., and Barton, J. K. “Electron transfer between metal complexes bound to DNA: variations in sequence, donor, and metal binding mode.” *Inorg. Chim. Acta* **297**, 88–97 (2000).
- [81] Delaney, S. “Oxidative DNA Damage by Long-Range Charge Transport.” Ph.D. thesis, 2004.
- [82] Olmon, E. D., Sontz, P. A., Blanco-Rodríguez, A. M., Towrie, M., Clark, I. P., Vlček, A., and Barton, J. K. “Charge Photoinjection in Intercalated and Covalently Bound  $[\text{Re}(\text{CO})_3(\text{dppz})(\text{py})]^+$ -DNA Constructs Monitored by Time-Resolved Visible and Infrared Spectroscopy.” *J. Am. Chem. Soc.* **133**, 13718–13730 (2011).